Full title: FMRFa receptor stimulated Ca^{2+} signals alter the activity of flight modulating central dopaminergic neurons in *Drosophila melanogaster*

Short title: FMRFa receptor modulates flight duration in *Drosophila melanogaster*

Preethi Ravi[1], Deepti Trivedi[1], Gaiti Hasan[1*]

[1] National Centre for Biological Sciences, Tata Institute of Fundamental Research, Bangalore 560065, India

* Corresponding Author: gaiti@ncbs.res.in

Abstract

Neuropeptide signaling influences animal behavior by modulating neuronal activity and thus altering circuit dynamics. Insect flight is a key innate behavior that very likely requires robust neuromodulation. Cellular and molecular components that help modulate flight behavior are therefore of interest and require investigation. In a genetic RNAi screen for G-protein coupled receptors that regulate flight bout durations, we earlier identified several receptors, including the receptor for the neuropeptide FMRFa (FMRFaR). To further investigate modulation of insect flight by FMRFa we generated CRISPR-Cas9 mutants in the gene encoding the *Drosophila* FMRFaR. The mutants exhibit significant flight deficits with a focus in dopaminergic cells. Expression of a receptor specific RNAi in adult central dopaminergic neurons resulted in progressive loss of sustained flight. Further, genetic and cellular assays demonstrated that FMRFaR stimulates intracellular calcium signaling through the IP_3R and helps maintain neuronal excitability in a subset of dopaminergic neurons for positive modulation of flight bout durations.

Author summary

Neuropeptides play an important role in modulating neuronal properties such as excitability and synaptic strength and thereby influence innate behavioral

outputs. In flying insects, neuromodulation of flight has been primarily attributed to monoamines. In this study, we have used the genetically amenable fruit fly, *Drosophila melanogaster* to identify a neuropeptide receptor that is required in adults to modulate flight behavior. We show from both knockdown and knockout studies that the neuropeptide receptor, *FMRFaR*, present on a few central dopaminergic neurons, modulates the duration of flight bouts. Overexpression of putative downstream molecules, the IP_3R, an intracellular Ca^{2+}-release channel, and CaMKII, a protein kinase, significantly rescue the flight deficits induced by knockdown of the *FMRFaR*. Our data support the idea that FMRFaR and CaMKII help maintain optimal membrane excitability of adult dopaminergic neurons required to sustain longer durations of flight bouts. We speculate that the ability to maintain longer flight bouts in natural conditions enhances the individual's capacity to search and reach food sources as well as find sites suitable for egg laying.

Introduction

Neuromodulation of animal behavior by neuropeptides is ubiquitous among vertebrates and invertebrates (1, 2). Unlike fast acting neurotransmitters, neuropeptides and their receptors influence neuronal activity and circuit dynamics by modulating presynaptic neurotransmitter release. The mechanisms for doing this include changes in ion channel and transporter function as well as regulation of

61 gene expression (1, 2). The neural action of neuropeptides can either be local or at
62 long distances by release into circulation and can influence intrinsic behaviors such
63 as feeding, mating, sleep and aggression (3, 4). An important and critical behavior
64 in flying insects is flight. Altered flight behavior, in particular the inability to
65 maintain long durations of flight bouts, can impinge on the fly's ability to
66 optimally search and reach food sources as well as sites suitable for egg laying.
67 Neuromodulation of insect flight has thus far been attributed primarily to biogenic
68 amines (5–7). A role for neuropeptide-based modulation of flight behavior has
69 remained largely unexplored.

70 In invertebrates, neuropeptides activate G-protein coupled receptors
71 (GPCRs) (8) followed by generation of soluble second messengers such as cAMP
72 (9–12) or inositol 1,4,5-trisphosphate (IP_3) (13–15). IP_3 binds to and activates the
73 endoplasmic reticulum (ER) localized Ca^{2+} channel, the IP_3 receptor (IP_3R),
74 resulting in release of calcium from ER-stores (16). Invertebrate neuropeptide
75 receptors that stimulate IP_3-mediated Ca^{2+} release include the Pigment Dispersing
76 Factor Receptor (PdfR) (14), FMRFaR (13–15) amongst others (8, 17). We
77 identified the PdfR and FMRFaR in a genetic screen for neuronal GPCRs that
78 regulate flight in *Drosophila* through IP_3-mediated Ca^{2+} release (14). Further
79 investigation of PdfR demonstrated a role for this receptor in both the developing
80 and adult flight circuit, though the identity of Pdf responsive neurons that affect

flight remained ambiguous (14). FMRFaR has been described earlier in the context of an escape response to intense light in *Drosophila* larvae (13) and the larval to pupal transition under nutrient-limiting conditions (15). Adult behaviors implicating the FMRFaR include startle-induced locomotor activity (18) and adaptive sleep following heat stress (19).

In the context of flight behavior, a neuronal requirement for IP_3-mediated Ca^{2+} release was initially described in flight deficient IP_3R mutants (20). Subsequent cellular and molecular studies identified a role for IP_3-mediated Ca^{2+} release in dopaminergic neurons during pupal stages, when the flight circuit matures (7). Interestingly though, flight deficits were also observed upon temporal knockdown of the *FMRFaR* exclusively in mature neurons (14). Thus far, flight deficits arising from adult specific reduction of IP_3/Ca^{2+} signaling have remained unexplored. Here we have investigated if FMRFaR mediated Ca^{2+} signaling is required for *Drosophila* flight by generating new CRISPR-Cas9 mediated mutants for the *FMRFaR*. Flight deficits arising from specific knockdown in adult dopaminergic neurons suggests a role for FMRFaR in modulating adult flight and implicate the IP_3R and possibly CaMKII as downstream signaling components. Genetic and cellular assays indicate that the FMRFaR on adult dopaminergic neurons helps maintain optimal membrane excitability which could potentially be required for synaptic release of dopamine.

Results

FMRFaR is required in dopaminergic neurons for maintenance of flight

The neuropeptide receptor, FMRFaR, was identified amongst other G-protein coupled receptors (GPCRS) as a positive regulator of *Drosophila* flight in a pan-neuronal screen, where genetic data supported IP_3R mediated Ca^{2+} signaling and store-operated calcium entry (SOCE) as the down-stream effectors of receptor activation (14). We confirmed these initial observations by RNAi mediated knockdown of the *FMRFaR* with another pan-neuronal GAL4 (*nSybGAL4*) in the central nervous system (CNS), followed by measurement of flight bout durations in tethered flies in response to a gentle air-puff. Unlike previous measurements where flight times were recorded for a maximum of 30 seconds (14), in the current study we monitored flight for 15 minutes (900 seconds), which allows for resolution of longer flight bout durations. Upon *FMRFaR* knockdown in *nSyb* positive neurons, significantly shorter flight bouts were observed as compared to controls (*FMRFaR*^{RNAi}/+, *nSyb*/+; Fig 1A). The efficacy of *FMRFaR* knockdown by the RNAi strain was confirmed in the adult CNS by pan-neuronal expression of the RNAi with *nSybGAL4*. A significant reduction in *FMRFaR* mRNA levels was observed (Fig 1B).

119 Similar to the pan-neuronal knockdown of *FMRFaR*, flight deficits were
120 also observed in flies with *FMRFaR*^{RNAi} targeted to a large number of dopamine-
121 synthesizing cells driven by *THGAL4* (Fig 1A). Because non-neuronal expression
122 of *THGAL4* has been documented (21), we tested GAL4s with restricted
123 expression in neurons (22). For this, we used the *THD* and *THCGAL4* driver lines
124 that mark non-overlapping subsets of central dopaminergic neurons (22).
125 Knockdown of *FMRFaR* using either the *THD1GAL4* or the *THD'GAL4* resulted
126 in flight deficits that were equivalent to the phenotype observed with *THGAL4*-
127 driven knockdown (Fig 1A, C, S1A Fig; *TH>FMRFaR*^{RNAi} vs.
128 *THD1>FMRFaR*^{RNAi} or *TH>FMRFaR*^{RNAi} vs *THD'>FMRFaR*^{RNAi} are not
129 significantly different from each other; $p>0.05$; Mann-Whitney U-test). However,
130 the *THDGAL4* strains are also known to express in some non-dopaminergic
131 neurons (22). To test the role, if any, of FMRFaR function in non-dopaminergic
132 neurons marked by *THDGAL4*s, expression of the *FMRFaR*^{RNAi} was blocked
133 specifically in TH-expressing neurons with the *THGAL80* transgene (23).
134 Importantly, the flight deficits observed in *THD>FMRFaR*^{RNAi} flies were reversed
135 upon introduction of *THGAL80* confirming that such flight deficits arose
136 exclusively from dopaminergic neurons marked by these GAL4s (Fig 1A; blue bar,
137 S1A Fig; blue bar). On the other hand, flies with knockdown of the *FMRFaR* using
138 the *THC1* or *THC'GAL4s* did not result in significant flight deficits, indicating that

139 dopaminergic neurons unique to *THD1* or *THD'GAL4* require FMRFaR mediated
140 signaling to regulate flight bout durations (S1A Fig). *THDGAL4* strains express in
141 central dopaminergic neurons comprising the Protocerebral Posterior Lateral 1
142 (PPL1) and Protocerebral Posterior Medial 3 (PPM3) clusters and these two
143 neuronal clusters are not marked by the *THC'GAL4* (7, 22). Furthermore, the
144 reduced flight deficit observed with *FMRFaR* knockdown in dopaminergic neurons
145 was not a consequence of overall reduction in motor activity because
146 *THD1>FMRFaR*^{RNAi} flies showed normal locomotor activity as compared to their
147 genetic controls (S1B Fig). Having identified the dopaminergic subsets where
148 FMRFaR is required for flight, subsequent experiments were performed with
149 *THD1GAL4* as the dopaminergic expression driver.

150 RNAi knockdown of *FMRFaR* with *nSybGAL4* reduced *FMRFaR* levels by
151 about 30% (Fig 1B). To further refine our understanding of the FMRFaR's role in
152 *Drosophila* flight, a complete knockout of the *FMRFaR* (*ΔFMRFaR*) was
153 generated by the CRISPR-Cas9 method (24). The strategy employed, removed
154 nearly 1.5 kb of the 1.6 kb coding region of *FMRFaR* (Fig 1D). Primers spanning
155 the *FMRFaR* locus (5'F+3'R) amplified only about ~400bp genomic fragment
156 from *FMRFaR* homozygous and heterozygous knockouts, thereby confirming
157 *FMRFaR* gene knockout (Fig 1D). Other primer pair combinations (5'F+5'R and
158 3'F+3'R) helped us distinguish between the homozygotes and heterozygotes.

159 Homozygous knockouts of the *FMRFaR* showed near complete loss of *FMRFaR*
160 mRNA as well as reduced flight bout durations as compared to the heterozygotes
161 (Fig 1E, F).

162 Next, we tested dopaminergic neuron specific knockout of *FMRFaR* by
163 expression of *UAScas9* in the genetic background of flies with ubiquitous
164 expression of guide RNAs that target the gene for *FMRFaR*
165 (*THD1>FMRFaR*^{dual}*;cas9*; see Materials and methods). Flies with knockout of the
166 *FMRFaR* in *THD1* cells flew for significantly shorter durations as compared to the
167 appropriate genetic controls (*FMRFaR*^{dual}*/+;cas/+* - Fig 1F; 4th bar in black and
168 *THD1/+* - Fig 1A; last bar in black; $p<0.01$; Mann-Whitney U-test) (Fig 1F). To
169 account for non-specific effects of *cas9* expression, we tested flies expressing only
170 the *cas9* transgene in *THD1* neurons (*THD1>cas9*). The flight deficit observed
171 with *FMRFaR* knockout in *THD1* cells was significantly different from
172 *THD1>cas9* flies (Fig 1F; *THD1>cas9* vs *THD1>FMRFaR*^{dual}*;cas9*; $p<0.01$;
173 Mann-Whitney U-test). The near identical flight deficits observed between
174 *FMRFaR* null flies and flies with *FMRFaR* knockout in *THD1* cells suggests that
175 modulation of flight bout duration by FMRFaR may derive solely from
176 dopaminergic neurons (Fig 1F; *THD1>FMRFaR*^{dual}*;cas9* vs *ΔFMRFaR*
177 Homozygous; $p>0.05$; Mann-Whitney U-test). To test this idea, we next
178 investigated whether *FMRFaR* is enriched in dopaminergic neurons of the brain.

179 **FMRFaR is present on dopaminergic neurons and is functionally active**

180 Owing to the lack of either an antibody for FMRFaR or GAL4 strains that
181 reliably mark FMRFaR expressing neurons, we chose to employ molecular and
182 functional assays to confirm the presence of FMRFaR on dopaminergic neurons.
183 Towards this end, we sorted adult brain dopaminergic neurons marked by *THGAL4*
184 driven *eGFP*, using fluorescence-activated cell sorting (FACS) and measured
185 transcript levels of a few selected genes. Two markers of dopaminergic neurons,
186 *ple* (encoding the enzyme Tyrosine Hydroxylase or TH) and *dDAT* (encoding a
187 dopamine transporter) were highly expressed in GFP +ve cells, confirming
188 homogeneity of the sorted population (Fig 2A). *FMRFaR* expression, as measured
189 by qPCR, was significantly enriched in *TH* expressing neurons (GFP +ve), whereas
190 expression of calcium signaling molecules like *dSTIM* and *dOrai* was similar in
191 dopaminergic and non-dopaminergic neurons (Fig 2A).

192 The presence of active FMRFaR on central dopaminergic neurons was tested
193 next. *THD1* neurons with expression of a genetically encoded calcium sensor,
194 *GCaMP6m* (25) were tested for receptor activation in adult brain explants and
195 calcium responses were specifically monitored from the PPL1 and PPM3 clusters,
196 previously implicated in the regulation of flight bout durations (Fig 1A, S1A Fig)
197 (7). Stimulation with one of the most abundantly expressed neuropeptide ligands of
198 FMRFaR, DPKQDFMRFa (henceforth referred to as FMRFa) (26, 27), resulted in

199 a slow calcium rise (Fig 2B, C, E, F). FMRFa peptide stimulated GCaMP6m
200 response was significantly attenuated upon knockdown of the *FMRFaR* using
201 either the RNAi or *FMRFaR*^{dual}*;cas9* (Fig 2B, C, E, F). Peptide stimulation of
202 *THD1* cells in the presence of a sodium channel inhibitor, 2 μM Tetrodotoxin
203 (TTX) resulted in calcium responses that were comparable to that obtained in the
204 absence of TTX (Fig 2D, E, F). This suggested that the rise in FMRFa-stimulated
205 Ca^{2+} is due to direct activation of the FMRFaR and not a consequence of synaptic
206 inputs from other neurons to the *THD1* neurons. Moreover, FMRFa stimulated
207 Ca^{2+} signals attenuated significantly upon knockdown of *itpr* in *THD1* marked
208 dopaminergic neurons (Fig. 2D, E, F). Taken together, these data suggest the
209 presence of FMRFaR on central brain dopaminergic neurons and that receptor
210 activation likely leads to Ca^{2+} release from the IP_3R.

211 **FMRFaR is required in adult dopaminergic neurons for sustained flight**

212 Pan-neuronal knockdown of the *FMRFaR* in an earlier study suggested a
213 requirement of the receptor both during pupal development and in adult
214 *Drosophila* neurons (14). To investigate the developmental stage(s) when
215 FMRFaR signaling is required in dopaminergic neurons for maintaining flight, the
216 TARGET (Temporal And Regional Gene Expression Targeting) system (28) was
217 used for stage-specific *FMRFaR* knockdown. This system employs a temperature

218 sensitive GAL80 element (*TubGAL80^{ts}*) which represses GAL4 expression at
219 18°C. At 29°C the GAL80^{ts} is inactivated, thus allowing GAL4 driven expression
220 of the UAS transgene. Flight durations of flies with *FMRFaR* knockdown in
221 dopaminergic neurons throughout development (29°C) were reduced to less than
222 300 seconds as compared to genetic controls that on average flew for about 600
223 seconds (Fig 3A, S2A Fig). Flies with knockdown of the *FMRFaR* in larval stages
224 displayed normal flight bouts (29°C Larval), whereas a modest reduction in flight
225 bout durations was observed with pupal knockdown (29°C Pupal) (Fig 3A).
226 Interestingly, knockdown of the *FMRFaR* in adult stages affected flight duration
227 maximally, with exacerbation of the flight deficit over time, such that flies with
228 knockdown for eight days flew for less than 150 seconds (29°C Adults) (Fig 3A).
229 In contrast, the control genotypes maintained at 29°C for the same adult period
230 could fly for an average of over 600 seconds (S2A Fig).

231 Next, we tested the ability of IP_3R overexpression to compensate for loss of
232 *FMRFaR* in adult dopaminergic neurons. Indeed, flight deficits observed with
233 *FMRFaR* knockdown in adults could be rescued to a significant extent by
234 simultaneous overexpression of an *itpr*$^{+}$ transgene (Fig 3A; blue bar; $p<0.01$;
235 Mann-Whitney U-test), but not another *UAS* transgene, *GCaMP6m* (Fig 3A;
236 orange bar; $p>0.05$; Mann-Whitney U-test). Rescue of *FMRFaR* knockdown by
237 overexpression of *itpr*$^{+}$ supports earlier findings that IP_3R-mediated Ca^{2+} release

238 functions downstream of FMRFaR (13) and is consistent with observations in Fig.
239 2D, E, F. Temporal and cell specific knockout of the *FMRFaR* with *FMRFaR*^{dual}
240 was attempted, but was not pursued because control flies with expression of *cas9*
241 in adult *THD1;TARGET* cells exhibit flight deficits when maintained at 29°C for 8
242 days (S2A Fig, last lane in pink). Consistent adult specific phenotypes were
243 observed with the *THD1GAL4* strain which has been used for subsequent
244 experiments.

245 The cellular basis for flight deficits arising from loss of *FMRFaR* in *THD1*
246 marked neurons was investigated next. Expression of endogenous TH and
247 membrane-bound GFP driven by *THD1GAL4* was visualized in the PPL1 and
248 PPM3 clusters of adult *Drosophila* brains at 8 days after knockdown of *FMRFaR*.
249 Both TH and GFP immunoreactivity appeared as in a control genotype, and there
250 was no apparent loss of dopaminergic neurons or their neurite projections (Fig 3B,
251 C, D, S2B Fig). Taken together these data suggest that the FMRFaR is required in
252 adult *THD1* neurons for sustaining flight bout durations. The increasing disability
253 to maintain flight bouts for longer durations upon manipulation of *FMRFaR* levels
254 in adult *THD1* neurons could likely be a consequence of increased RNAi
255 expression over time.

256 **CaMKII in dopaminergic neurons is required for flight**

257 Downstream signaling mechanisms that require FMRFaR activation in
258 *THD1* dopaminergic neurons were investigated next. There is evidence
259 demonstrating that FMRFa evoked modulation of excitatory junction potentials
260 (EJPs) at *Drosophila* neuro-muscular junctions are dependent on the protein
261 kinase, CaMKII (13, 29). Hence, we tested whether overexpression of wild-type
262 *CaMKII* (*WT-CaMKII*) in dopaminergic cells rescued the deficit in flight bout
263 durations observed upon reduced FMRFaR signaling. Overexpression of *WT-*
264 *CaMKII* during pupal stages was insufficient to rescue flight deficits in adults (Fig
265 4A). However overexpression of *WT-CaMKII* in adults modestly rescued
266 $FMRFaR^{RNAi}$ induced flight deficits on day 4, 6 and 8 (Fig 4A, S2A Fig -
267 *THD1;TARGET* controls and S3A Fig – *WT-CaMKII/+;*$FMRFaR^{RNAi}$*/+* controls).
268 It should be noted that overexpression of *WT-CaMKII* in adult dopaminergic
269 neurons also reduced the duration of flight bouts (S3A Fig; orange bars),
270 suggesting that CaMKII levels need to be tightly regulated in adult dopaminergic
271 neurons for maintenance of flight (see Discussion). Lack of robust rescue by
272 CaMKII of flight deficits in *FMRFaR* knockdown flies may in part arise from an
273 imbalance between levels of FMRFaR and CaMKII in *THD1* neurons. Rescue with
274 the constitutively active form of CaMKII ($CaMKII^{T287D}$) was not attempted
275 because expression of $CaMKII^{T287D}$ in adult *THD1* neurons resulted in strong flight
276 deficits (S3A Fig; maroon bars). Reduced neuronal excitability by overexpression

277 of the mutant transgene, *CaMKII*^{T287D} in larval neurons has been observed
278 previously where it elicited behavioral deficits, presumably via modulation of
279 potassium currents (30) (also see discussion). Overall the partial rescue of flight
280 deficits in the *FMRFaR* knockdown animals by expression of a *WT-CaMKII*
281 transgene indicates a genetic interaction between them.

282 To test directly if CaMKII is required in dopaminergic neurons to modulate
283 flight bout durations, we expressed a synthetic peptide inhibitor of CaMKII (*Ala*)
284 (31) in dopaminergic cells of interest. Ala is a peptide analog of the CaMKII
285 autoinhibitory domain that can bind to the catalytic domain of CaMKII, thereby
286 functioning as an exogenous inhibitor. Inhibition of CaMKII in pan-dopaminergic
287 (*TH*) or the subset dopaminergic neurons (*THD1*) resulted in flies with
288 significantly reduced durations of flight bouts (Fig 4B). Knockdown of *CaMKII*
289 with a *CaMKII*^{RNAi} also elicited a significant reduction of flight bout durations
290 (S3B Fig). Inhibition of CaMKII activity by the *Ala* peptide in *THD1* neurons did
291 not affect their general locomotor ability, indicating that CaMKII function in
292 *THD1* neurons is likely to be flight specific (S3C Fig). Additionally, TARGET
293 experiments demonstrated that *THD1*-driven expression of *Ala* specifically in
294 either pupal or adult stages significantly compromised the duration of flight bouts,
295 as compared to genetic controls (Fig 4C, S2A Fig - *THD1;TARGET* controls, S3D
296 Fig - *Ala/+* controls). Given that CaMKII is involved in several developmental

297 processes, for example, axon terminal growth (32), a pupal requirement for
298 CaMKII is not surprising. Maximal reduction in flight bout duration was observed
299 in flies wherein CaMKII was inhibited by *Ala* peptide expression in *THD1* cells for
300 8 days as adults (Fig 4C).

301 These data support a role for CaMKII activity in the *THD1* subset of
302 dopaminergic neurons in the specific context of maintaining flight bout durations.
303 Similar to *FMRFaR* knockdown, CaMKII inhibition with *Ala* in adult neurons did
304 not affect levels of *TH* mRNA (S3E Fig). Thus, unlike previous findings where
305 reduced Ca^{2+} signaling in pupal dopaminergic neurons resulted in reduced
306 expression of the gene encoding TH (*ple* or *TH*) (6, 7), FMRFaR and CaMKII in
307 adult dopaminergic neurons appear to modulate flight by an alternate cellular
308 mechanism.

309 To test if CaMKII activity affects FMRFaR induced Ca^{2+} release, *THD1*
310 neurons expressing *Ala* peptide were stimulated with the FMRFa peptide. FMRFa-
311 stimulated cellular calcium responses were not affected by *Ala* expression in *THD1*
312 neurons (Fig 4D, E, F). These data suggest that the function of CaMKII is either
313 downstream or parallel to FMRFaR induced Ca^{2+} release.

314 The ability of FMRFa to activate CaMKII in *Drosophila* central brain
315 neurons was tested next by immunostaining for pCaMKII, a CaMKII modification

316 that occurs upon prolonged calcium elevation in the cell (30, 33). For technical
317 reasons, this immunostaining was performed on primary neuronal cultures from
318 larvae, wherein we overexpressed the *FMRFaR*$^{+}$ in all *nSybGAL4* positive neurons
319 (34). In addition, the same neurons were marked with *mCD8GFP* to normalize the
320 pCaMKII signal and to account for variability in strength of expression of the
321 overexpressed *FMRFaR*$^{+}$. A significant increase in pCaMKII/GFP staining was
322 observed upon stimulation of larval *nSyb>FMRFaR*$^{+}$*;mCD8GFP* positive neurons
323 with FMRFa as compared to cells with solvent addition (S3F-H Fig). These data
324 support the idea that FMRFa stimulated Ca^{2+} release activates CaMKII in central
325 brain neurons. Even though a direct test for FMRFa-stimulated CaMKII activation
326 in *THD1* neurons has not been possible so far due to technical reasons, the ability
327 of *WT-CaMKII* to partially rescue the flight deficit in *FMRFaR* knockdown
328 animals (Fig 4A), taken together with these cellular data suggest that CaMKII may
329 function downstream of FMRFaR signaling. Nevertheless, an FMRFaR-
330 independent and parallel role for CaMKII in *THD1* neurons remains possible. The
331 underlying cellular basis for the flight deficits observed upon *FMRFaR* knockdown
332 and *Ala* expression in dopaminergic neurons was investigated next.

333 **FMRFaR and CaMKII modulate calcium entry and membrane potential in**
334 **central dopaminergic neurons**

335 To measure neuronal activity of *THD1* neurons, we tested their response to a
336 depolarizing stimulus. *Ex vivo* brain preparations from *THD1* marked
337 dopaminergic neurons were stimulated with 70 mM KCl, a condition known to
338 raise the resting membrane potential and activate voltage-gated calcium channels
339 on the plasma membrane (35). The stimulation was followed by optical
340 measurements of calcium dynamics. Firstly, using the TARGET system, we
341 expressed *GCaMP6m* in *THD1* marked cells, specifically in adults. Animals reared
342 at 29°C for 8 days (also the time corresponding to maximal flight loss upon
343 *FMRFaR* knockdown or *Ala* expression; Fig 3A, 4C), were used in these
344 experiments. Robust Ca^{2+} elevations were observed in *THD1* marked cells from
345 control animals upon addition of KCl (Fig 5A-D; black trace). Ca^{2+} responses from
346 neurons with either *FMRFaR* knockdown or *Ala* expression, were however
347 significantly reduced as compared to controls (Fig 5A-D; red and blue traces).
348 Similar experiments on *ex vivo* brains obtained after *FMRFaR* knockdown in
349 adults for 2 days, exhibit a minimal decrease in Ca^{2+} responses upon depolarization
350 with KCl, in agreement with their weak flight deficits (S4A-C Fig, Fig 3A). These
351 data suggest that FMRFaR and CaMKII help maintain normal cellular responses to
352 changes in membrane excitability in *THD1* neurons. Interestingly, in the *FMRFaR*
353 knockdown condition, most cells exhibit a dampened Ca^{2+} response (Fig 5D, 2nd
354 row - pink arrow), but a few cells responded normally (Fig 5D, 2nd row - yellow

355 arrow). Their normal response may be due to insufficient receptor knockdown.
356 Alternately all *THD1* marked cells might not express the FMRFaR (see
357 discussion).

358 **Increased membrane excitability can partially compensate for loss of**
359 **FMRFaR and CaMKII function**

360 Based on the reduced Ca^{2+} elevation upon depolarization with KCl, observed
361 in *THD1* marked dopaminergic neurons of flies with either *FMRFaR* knockdown
362 or CaMKII inhibition, we hypothesized that such neurons might have reduced
363 membrane excitability. To ascertain if reduced FMRFaR signaling indeed alters the
364 ability of *THD1* neurons to undergo membrane depolarization, a genetically
365 encoded fluorescent voltage indicator, *Arclight* (36), was expressed in
366 dopaminergic neurons of *THD1GAL4*. Stimulation of 8 day old adult brains with
367 KCl showed a robust change in Arclight fluorescence corresponding to neuron
368 depolarization (Fig 6A-D; black trace). As proof of concept, expression of *Kir2.1*
369 in *THD1* cells for 2 days nearly abolished KCl induced membrane depolarization
370 (S5A-C Fig; blue trace). Dopaminergic neurons with *FMRFaR* knockdown for 8
371 days displayed a significantly reduced ability to depolarize after KCl addition (Fig
372 6A-D; red trace). As was observed previously (Fig 5D), membrane depolarization
373 induced changes in Arclight fluorescence were attenuated in most *THD1* neurons
374 (Fig 6D, 2nd row; pink arrow), while few responded like controls (Fig 6D, 2nd row;

375 yellow arrow). Similar experiments with adult brains at 2 days exhibit equivalent
376 changes in membrane potential in both control and with *FMRFaR*^{RNAi}, in
377 agreement with the weaker flight deficits of 2d old flies with *FMRFaR* knockdown
378 (S5A-C, Fig 3A).

379 Because knockdown of *FMRFaR* reduced KCl induced Ca^{2+} entry in
380 dopaminergic neurons (Fig 5A-D), attenuated membrane depolarization (Fig 6A-
381 D) and correlated with shortened flight bout durations (Fig 3A), we hypothesized
382 that FMRFaR function is likely required to maintain optimal excitability in these
383 neurons. Consequently, increasing neuronal excitability might compensate for
384 reduced FMRFaR function and thereby rescue the flight deficits observed in
385 *FMRFaR* knockdown flies. To test this idea, we introduced a temperature sensitive
386 cation channel, *dTrpA1* (37) in flies with adult specific *FMRFaR* knockdown.
387 Activation of the dTrpA1 calcium channel can compensate in part for reduced Ca^{2+}
388 entry through voltage–gated channels (15, 38). Indeed, expression of *dTrpA1*
389 significantly improved the maintenance of flight bouts in 6 and 8 day old *FMRFaR*
390 knockdown adults (Fig 6E, S2A Fig - *THD1;TARGET* controls and S5D Fig –
391 *TrpA1/+;FMRFaR*^{RNAi}*/+* controls). Likewise, expression of *NaChBac* (a bacterial
392 sodium channel) (39), moderately alleviated the near loss of flight observed with
393 *Ala*-dependent CaMKII inhibition in 6 and 8 day old adults (S5E, F Fig).
394 Expression of another UAS element (*GCaMP6m*) in the background of *FMRFaR*

395 knockdown or *Ala* expression did not rescue the loss of flight (S5F Fig; green bar,
396 as compared to Fig 3A; orange bar – 8 days as Adults at 29°C; p>0.05; Mann-
397 Whitney U-test). Expression of just the *TrpA1* or the *NaChBac* transgenes in adult
398 dopaminergic neurons also affected flight bout durations, supporting the idea that
399 optimal activity of ion channels in *THD1* marked adult dopaminergic neurons is
400 required for their normal function (S5D, F Fig). Taken together, these data
401 demonstrate that FMRFaR helps maintain optimal excitability of flight bout
402 extending central dopaminergic neurons.

403 **Membrane excitability and synaptic vesicle recycling in dopaminergic**
404 **neurons is essential for sustained flight**

405 To directly test if changes in membrane excitability of *THD1* neurons,
406 affects their ability to modulate flight bout durations, we expressed transgenes that
407 encode ion channel specific tethered-toxins in adult *THD1* neurons. Expression of
408 such toxins, in *Drosophila* neurons, inhibits voltage-gated ion channels thereby
409 altering neuronal excitability and behavior (40). Expression of *PLTXII*, a toxin that
410 targets the presynaptic calcium channel, *cacophony*, in adult *THD1* neurons
411 significantly impaired maintenance of flight bouts from as early as 2 days of
412 transgene expression (Fig 7A, S6A Fig). By 6 days, just 20% of the flies survived
413 *PLTXII* expression and hence flight measurements were recorded only up to 4 days
414 at 29°C (Fig 7A, S6A Fig). Similarly, blocking potassium channels by expression

415 of *κ-ACTX-Hv1c*, in adult dopaminergic neurons also compromised the duration of
416 flight bouts to a significant extent (Fig 7B, S6A Fig). Approximately 60% lethality
417 was observed with *κ-ACTX-Hv1c* expression in adult *THD1* neurons for 6 days. It
418 is not surprising that we observe lethality with the *PLTXII* and *κ-ACTX-Hv1c*
419 transgenes as pan-neuronal expression of each of these toxins has previously been
420 reported to result in lethality (40). Next, adult specific expression of *δ-ACTX-*
421 *Hv1a*, a toxin that inhibits inactivation of voltage-gated sodium channels (encoded
422 by the gene *para*), in *THD1* neurons also reduced flight bout duration in adult flies
423 after 4 days of transgene expression (Fig 7C, S6A Fig). Furthermore, by
424 immunostaining for endogenous TH, we confirmed that dopaminergic neurons
425 were intact under these conditions (S6B Fig). Taken together, these data suggest
426 that the membrane excitability of flight modulating *THD1GAL4* marked central
427 dopaminergic neurons must be tightly controlled for maintenance of long flight
428 bouts.

429 We hypothesized that changes in membrane excitability are likely to affect
430 the release of dopamine containing synaptic vesicles from *THD1* neurons. A
431 temperature-sensitive mutant transgene for dynamin (*UAS-Shibire*^{ts} or *Shi*^{ts}) (41)
432 was used to block synaptic vesicle recycling by shifting flies transiently to the non-
433 permissive temperature of 30˚C. Indeed, when synaptic vesicle recycling was
434 inhibited in *THD1* neurons of adult flies, reduced flight bout durations were

435 observed as compared with controls (Fig 7D). Flies of the same genotype
436 (*THD1>Shi*^{ts}) maintained at 22°C throughout showed normal flight bout durations
437 (Fig 7D). Thus acute manipulation of synaptic function of adult *THD1* neurons
438 affects the maintenance of flight bout duration in the tethered flight paradigm.
439 Finally, we tested requirement for the neurotransmitter, dopamine in *THD1*
440 neurons, for modulating the duration of adult flight bouts. Adult-specific
441 expression of an RNAi transgene for the dopamine-synthesizing enzyme Tyrosine
442 Hydroxylase (*TH*^{RNAi}; (42)) in *THD1* neurons significantly impaired the
443 maintenance of longer flight bouts from as early as 2 days of *TH*^{RNAi} expression
444 (Fig 7E), suggesting that dopamine release from synapses of *THD1* neurons is
445 required for maintaining longer flight bouts.

446 **Discussion**

447 In this study we demonstrate that the FMRFaR and CaMKII signaling in
448 specific central dopaminergic neurons of the adult *Drosophila* brain helps maintain
449 optimal membrane excitability (Fig 5A-D, 6A-D). Previous work by our group
450 demonstrated that loss of IP_3R mediated Ca^{2+} signaling in central dopaminergic
451 neurons during pupal stages similarly affects flight circuit function in adults (6, 7).
452 In parallel, neuropeptidergic modulation of flight by the Pdf receptor was
453 investigated, but the exact class of neurons that required this receptor or the
454 downstream effectors remained elusive (14). For the first time, we describe here a

455 neuropeptidergic signaling mechanism in adult brain neurons that is required for
456 sustained flight (S6C Fig). Our data support a model where FMRFa-modulated
457 activity in central dopaminergic neurons belonging to the PPL1 and PPM3 clusters
458 extends the duration of flight bouts, a behavior that is likely to have significant
459 effects on optimal sourcing of nutrients, finding sites for egg laying and identifying
460 mates in the wild.

461 The role of neuropeptide signaling in modulating animal behavior is well
462 documented (2, 4). Indeed, rescue of flight deficits by overexpression of the cation
463 channel *TrpA1* in dopaminergic neurons of *FMRFaR* knockdown flies directly
464 addresses the importance of peptide driven neuronal excitability, for flight
465 behavior (Fig 6E). Reduced cellular responses to a depolarizing stimulus observed
466 upon *FMRFaR* knockdown in *THD1* neurons may arise from functional
467 modification, possibly by CaMKII, of plasma membrane resident ion channels, or
468 their expression levels (Fig 5A-D, 6A-D). However, our data do not exclude other
469 kinases or modifiers as functioning downstream of the FMRFaR. We predict that
470 FMRFaR in dopaminergic neurons is a key neuromodulator of membrane
471 excitability which stimulates release of dopamine containing synaptic vesicles. In
472 fact, stimulation of synaptic transmission downstream of FMRFaR activation has
473 been described previously in *Drosophila* larval neuromuscular junctions (13).
474 Though we have not tested synaptic vesicle release directly upon FMRFaR

475 stimulation, our data support an essential role for synaptic transmission and
476 dopamine synthesis in adult dopaminergic neurons for maintenance of flight bout
477 durations (Fig 7D, E). Identification of the precise ion channels that are affected by
478 FMRFaR signaling, leading to changes in membrane excitability and very likely
479 synaptic transmission in flight modulating dopaminergic neurons, needs further
480 investigation.

481 Multiple FMRFa peptides exist in *Drosophila* (26, 27). Cells positive for
482 FMRFa peptides have been characterized in the *Drosophila* central nervous system
483 using antisera specific to some of the FMRFa peptides (43–46). Immunostaining of
484 adult brains, especially against the peptide, DPKQDFMRFa (also used in this
485 study) have revealed extensive neuronal varicosities in the anterior and lateral
486 regions of the protocerebrum (45, 46). It is hence conceivable that FMRFa released
487 through these projections activates the FMRFaR on the anatomically proximal
488 PPL1 and PPM3 clusters of dopaminergic neurons. The PPL1 neurons are known
489 to innervate the superior protocerebrum, a region considered to function at the
490 interface of olfactory input and motor output modules of the brain (47). Thus
491 activation of the FMRFaR on dopaminergic neurons might stimulate dopamine
492 release, which could then reinforce a dopaminergic circuit, required for sustained
493 flight. Furthermore, co-expression of the dopamine synthesizing enzyme Tyrosine
494 Hydroxylase (TH) in a few neurons marked by an *FMRFaGAL4* (48), suggests the

495 existence of an autocrine signaling mechanism within the flight modulating
496 dopaminergic neurons. This idea is supported by recent studies of single cell
497 sequencing of *Drosophila* neurons where FMRFa transcripts were seen in a small
498 number of central brain dopaminergic neurons (49, 50). Interestingly, a recent
499 report from *Manduca* demonstrated that an FMRFa positive neuron lies at the
500 center of a putative sensory-motor circuit for integration of olfactory stimuli with
501 wing movements during flight (51). The natural context in which FMRFa release is
502 triggered for modulation of flight in *Drosophila* remains to be identified.
503 Neuromodulatory signals from other receptors in central dopaminergic neurons is
504 also a possibility and would widen the scope of sensory inputs received by these
505 cells for integration with flight behavior.

506 FMRFaR activation by the peptide DPKQDFMRFa stimulates intracellular
507 Ca^{2+} release through the IP_3R (Fig 2D-F) (13) and enhances synaptic transmission
508 at the larval neuromuscular junction and thereby modulates muscle contraction (13,
509 29, 46). Previous work from our lab has demonstrated that in *Drosophila* neurons,
510 subsequent to intracellular Ca^{2+} release, cytosolic calcium is further elevated by
511 store-operated Ca^{2+} entry (SOCE) through dOrai (52). Thus, we predict that the
512 rise in Ca^{2+} we see upon FMRFa stimulation of *THD1* neurons could possibly be a
513 combination of both IP_3R mediated Ca^{2+} release and SOCE. Rescue of flight
514 deficits in the *FMRFaR* knockdown flies by an *itpr*$^+$ transgene (Fig 3A) and loss of

515 peptide induced Ca^{2+} rise in an *itpr* knockdown background (Fig 2D-F) support the
516 idea that IP_3R-mediated Ca^{2+} release is likely downstream of FMRFaR activation.
517 Activation of overexpressed IP_3Rs in the *FMRFaR* knockdown condition might
518 occur through alternate receptors. It is also possible that overexpression of the IP_3R
519 allows for more ER-Ca^{2+} release from the residual FMRFaRs after RNAi
520 knockdown. Thus, in the context of flight as well, FMRFaR signaling in
521 dopaminergic neurons appears to function upstream of IP_3R-mediated Ca^{2+} release
522 (Fig 2D-F, 3A). The adult requirement of FMRFaR on dopaminergic neurons
523 supports a primary role for this receptor in mature neurons for modulation of flight,
524 but not as much for maturation of the flight circuit in pupal stages (Fig 3A). In
525 contrast, the dFrizzled2 receptor, which also functions upstream of the IP_3R in
526 central dopaminergic neurons, was shown to be required exclusively during the
527 pupal stages, albeit in a different dopaminergic cluster of the brain (6). These
528 observations support the existence of specific receptors that stimulate IP_3-mediated
529 Ca^{2+} release and function either during flight circuit maturation in pupae or in a
530 neuromodulatory role in adults, to influence flight circuit dynamics. A range of
531 flight deficits in IP_3R mutants with differing allelic strength support this idea (20).

532 As described previously by other groups in larval motor neurons and in
533 larval neuromuscular junctions (13, 29), our genetic and cellular data also suggests
534 that CaMKII might be a downstream effector of FMRFaR signaling in neurons

535 (Fig 4A, S3F-H Fig). Although we have shown increased pCaMKII
536 immunostaining in larval CNS neurons upon FMRFa stimulation (S3F-H Fig),
537 direct activation of either CaMKII or other Ca^{2+} dependent kinases by FMRFa in
538 adult *THD1* neurons, remains to be tested rigorously. CaMKII, thus far has been
539 known to contribute to synaptic plasticity in the context of learning and memory
540 (53, 54). Our data, for the first time, demonstrate that CaMKII is required in
541 dopaminergic neurons for maintenance of *Drosophila* flight over periods of several
542 minutes, possibly by modulating neuronal firing during flight. Multiple
543 mechanisms for CaMKII dependent modulation of membrane excitability have
544 been described in *Drosophila* such as phosphorylation of the potassium channel,
545 Eag, leading to an increase in the Eag current (55). In another study, CaMKII
546 dependent phosphorylation of the Ca^{2+} activated potassium channel binding
547 protein, Slob was shown to favor its binding to 14-3-3, that eventually altered the
548 voltage sensitivity of slowpoke channels (56). In both cases, CaMKII acted as a
549 negative regulator of neuronal excitability, and support our data demonstrating
550 flight deficits observed upon overexpression of *WT-CaMKII* and $CaMKII^{T287D}$
551 (S3A Fig). However, the more interesting and compelling explanation for our data
552 demonstrating reduced KCl-induced depolarization upon CaMKII inhibition by
553 *Ala* comes from *in vitro* work that has described a role for CaMKII in decelerating
554 the inactivation of voltage sensitive calcium channels, thereby enhancing

555 transmitter release (57). This was however shown to be independent of its kinase
556 activity. More recently, there is evidence to suggest CaMKII-dependent activation
557 of transcription factors in *Drosophila* neurons (58, 59). Hence, the possibility of
558 transcriptional regulation of voltage-gated membrane channel genes by CaMKII
559 cannot be excluded and needs further investigation.

560 **Materials and Methods**

561 **Fly rearing and stocks**

562 *Drosophila* strains used in this study were maintained on cornmeal media,
563 supplemented with yeast. Flies were reared at 25°C, unless otherwise mentioned.
564 WT strain of *Drosophila* used was Canton-S. The fly lines *nSybGAL4* (BL51635),
565 *UASFMRFaR*^{RNAi} (BL25858), *UAScas9* (BL54593), *UASdTrpA1* (BL26263),
566 *UASNaChBac* (BL9468), *UASKir2.1* (BL6595), *UASGCaMP6m* (BL42748),
567 *UASArclight* (BL51057), *UASmCD8GFP* (BL5130), *UASAla* (BL29666), *UASWT-*
568 *CaMKII* (BL29662), *UASCaMKII*^{T287D} (BL29664), *UASTH*^{RNAi} (BL25796),
569 *UASDicer* (BL24648) were obtained from Bloomington *Drosophila* Stock Centre
570 (BDSC). The *UASitpr*^{RNAi} (1063-R2) strain was from National Institute of Genetics
571 (NIG) and the *UASCaMKII*^{RNAi} (v38930) was from Vienna Drosophila Resource
572 Center (VDRC). A strain with two copies of *TubGAL80*^{ts} on the second
573 chromosome was generated by Albert Chiang, NCBS, Bangalore, India, and has

been used for all TARGET experiments. The dopaminergic GAL4 driver, *THGAL4* (21) and the *THGAL80* strain (23) were kindly provided by Serge Birman (CNRS, ESPCI Paris Tech, France). All the TH subset GAL4s (*THD1, THD', THC1, THC'*) were a gift from Mark N Wu (Johns Hopkins University, Baltimore) (22). The *UASeGFP* transgene was provided by Michael Rosbash (Brandeis University, Waltham, MA). The *UASShi*^{ts} strain was obtained from Toshihiro Kitamoto (University of Iowa, Carver College of Medicine, Iowa City). The *UAS-toxin* fly strains have been described earlier (40) and were obtained from Brian McCabe (EPFL Brain Mind Institute, Lausanne, Switzerland). The generation and use of *UASitpr*$^{+}$ transgene has been described earlier (15, 60). The *UASFMRFaR*$^{+}$ strain was generated in the lab (unpublished). Standard fly genetics were followed for making strains and recombinants.

Temperature shift experiments were performed as described below. Briefly, larvae, pupae or adults were maintained at 18°C and transferred to 29°C only at the stage when the *UAS-transgene* needed to be expressed. Firstly, as a control, flies of the genotype *THD1;TARGET>UAS-transgene* were maintained throughout at 18°C, a condition where the *UAS-transgene* expression is suppressed (labeled as '18°C' in figures). To observe maximum effect, flies of the same genotype were grown at 29°C throughout development and as adults (labeled '29°C'). For larval specific knockdown, animals of the desired genotypes developed at 29°C from embryos to

594 the wandering larval stage, following which they were maintained at 18°C till the
595 time when they were tested for flight (labeled as '29°C Larval'). Likewise, for
596 pupal specific knockdown, wandering third instar larvae were shifted from 18°C to
597 29°C. Pupae developed at 29°C and were transferred to 18°C, soon after eclosion
598 (labeled as '29°C Pupal'). In case of adult specific knockdown, larval and pupal
599 development continued at 18°C. Following this, adult flies were maintained at
600 18°C for two days post eclosion and then transferred to 29°C and used for
601 experiments at 1, 2, 4, 6 or 8 days after transfer (labeled as '29°C Adult').

602 **Generation of a knockout for *FMRFaR* using the CRISPR-Cas9 system**

603 To generate a *FMRFaR* null allele, we used the CRISPR-Cas9 methodology (61–
604 65). Two guide RNAs (gRNAs) were designed, at the 5' and 3'ends of the gene at
605 the following sequences: (sg1-GGGAGCCATGAGTGGTACAGCGG, sg4-
606 GATCTCTGCATTTCGCGGGCGGG) so as to delete ~1.5 kb from the coding
607 region of the 1.6 kb gene. A gRNA dual transgenic fly (*FMRFaR*^{dual}) was made
608 first (24). *FMRFaR*^{dual} transgenic males were mated with *Act5c-Cas9* virgins (66).
609 From the F1 progeny obtained, 16 were screened by PCR for the deletion. Because
610 all flies tested were positive for the deletion, 4 F1 flies were individually crossed to
611 balancers and 30 F2 progeny were screened for the deletion. Progeny, that were
612 positive for deletion and negative for presence of dual gRNA (total 6 F2s), were
613 maintained as stable lines. The deletion was confirmed by sequencing of the DNA

614 from the *FMRFaR* knockout flies. The following primers were used for
615 confirmation of deletion - 5'F: GACATAGTCATCAGGTGCTC, 5'R:
616 TGCACCTCCGTGTGGTTAAG, 3'F: GAACAACGGCGATGGAACTC, 3'R:
617 GGTGCTCTAAGTCAACCCCT. For tissue specific deletions of *FMRFaR* gene, a
618 fly strain containing *FMRFaR*^{dual} and *UAScas9* was made and subsequently mated
619 with GAL4 strains of interest.

620 **Single flight Assay**

621 Single flight tests were performed on adult flies 3-5 days post eclosion, unless
622 specified differently. Flies were anaesthetized on ice for 2-3 minutes and then
623 tethered using nail polish applied to the end of a thin metal wire. The tether was
624 glued onto the region between the neck and thorax of adult flies. A gentle mouth
625 blown air-puff was delivered to test for flight response. Flight time in tethered
626 condition was recorded for a maximum of 15 minutes. In three independent
627 batches of 10, a minimum of 30 flies were tested for each genotype. All control
628 genotypes tested were obtained by crossing the GAL4 or UAS strain of interest to
629 the wild-type strain, *Canton-S*. Raw data was plotted as box and whisker plots
630 using Origin (OriginLab, Northampton, MA) software. Each bar represents 25th to
631 75th percentile. The solid diamond and horizontal line within the bars indicate
632 mean and median, respectively. Individual values are shown as open diamonds.

633 **Locomotor Assay**

634 Locomotor activity was measured by modifying a previously published protocol
635 (67). Briefly, locomotor activity of 4-6 day old singly housed virgin males was
636 tested in a circular chamber of diameter 4 cm. The chamber was placed on a sheet
637 containing a specific pattern. Single flies were aspirated into each chamber and
638 allowed to acclimatize for 5 minutes. Each fly was monitored separately for the
639 number of times it crossed each line in the pattern, over a period of 10 seconds. For
640 every experiment, six single flies were tested sequentially for the span of 10
641 seconds. This was repeated 5 times, i.e. we measured locomotor activity of every
642 single fly five times in blocks of 10 seconds, so as to randomize activity
643 measurements during the experimental time. Total locomotor activity is
644 represented as the sum total of the number of lines crossed by each fly over the
645 experimental duration of 50 seconds (plotted as Locomotor Activity Units). A
646 minimum of 25 flies were tested from each genotype.

647 ***Ex vivo* live imaging of adult brains**

648 Adult brains were dissected in adult haemolymph-like solution (AHL) (68) and
649 embedded in ~10 µl of 1% low melt agarose (Invitrogen) with anterior side facing
650 upwards. Brains were then bathed in 100 µl AHL until imaging. Images were
651 obtained on an Olympus FV1000 inverted microscope (Olympus Corp., Japan) in
652 time lapse mode using the 20X objective. Both GCaMP6m and Arclight signals

653 were captured using the 488 nm excitation laser line. Fifty frames of basal activity
654 were recorded, followed by stimulation with either 5 μM Peptide (DPKQDFMRFa,
655 NeoBioLab, Massachusetts, USA) or 70 mM KCl. A minimum of 5 brain explants
656 were imaged for every experimental condition.

657 Raw fluorescence data for regions of interest were extracted using the Time Series
658 Analyser plugin in Image J 1.47v. Change in fluorescence, ΔF/F was calculated
659 using the following formula for each time (t): $\Delta F/F = (F_t - F_0)/F_0$, where F_0 is the
660 average basal fluorescence of the first 10 frames. Area under the curve and Peak
661 ΔF/F was calculated using Microsoft Excel considering all frames post-stimulation.
662 Values were plotted as box plots.

663 **Sorting of adult neurons by FACS**

664 Twenty adult CNS (*THGAL4>eGFP*) were dissected in cold Schneider's medium
665 (#21720-024, Life Technologies) followed by ~45 minutes incubation in an
666 enzymatic solution containing 0.75 μg/μl of Collagenase (Sigma-Aldrich) and 0.40
667 μg/μl Dispase (Sigma-Aldrich). Brain lysates were then spun at 3000 rpm for 3
668 minutes. The supernatant was discarded and the pellet was resuspended in cold
669 Schneider's media. Single cell suspensions were obtained by gentle tituration and
670 then passed through a 40 μm mesh filter. Fluorescence-activated cell sorting
671 (FACS) of samples was carried out as described earlier (7). A minimum of 4

672 biological replicates were sorted and ~10,000 GFP +ve and GFP -ve cells were
673 collected separately in TRIzol Reagent (Life Technologies) for RNA isolation.

674 **RNA isolation and qPCR**

675 Total RNA was extracted from sorted cells or dissected adult CNS using TRIzol
676 RNA extraction protocol (Ambion, ThermoFischer Scientific). In case of dissected
677 CNS, a minimum of three biological replicates, each containing 5 brains, was used
678 per genotype. Approximately 500 ng of RNA was then used for DNAse treatment
679 and first strand cDNA synthesis. Quantitative real-time PCR was performed on
680 ABI7500 fast machine (Applied Biosystems) using Kapa SYBR FAST qCR
681 Master mix (KAPA Biosystems, Wilmington, MA). *rp49* was used as an internal
682 control to quantify relative levels of the target transcripts. qPCR values are
683 represented as normalized fold change of mRNA transcripts of the indicated genes.
684 In case of sorted cells, normalized mRNA levels of genes in GFP -ve cells have
685 been plotted relative to the GFP +ve population. Every qPCR run was followed by
686 a melt curve analysis to confirm primer specificity. The following formula was
687 used to calculate fold change:

688 Fold change = $2^{-\Delta\Delta Ct}$, where, $\Delta\Delta Ct = (Ct(_{\text{target gene}})-Ct(_{rp49}))_{Experimental} - (Ct(_{\text{target gene}})-$
689 $Ct(_{rp49}))_{Control}$

690 Sequences of primers used are as follows:

691 *rp49*:

692 Forward- CGGATCGATATGCTAAGCTGT

693 Reverse- GCGCTTGTTCGATCCGTA

694 *FMRFaR*:

695 Forward- GTGCGAAAGTTACCCGTCG

696 Reverse- TAATCGTAGTCCGTGGGCG

697 *TH* (*ple*):

698 Forward- GTTGCAGCAGCCCAAAAGAAC

699 Reverse- GAGACCGTAATCATTTGCCTTGC

700 *dSTIM*:

701 Forward- GAAGCAATGGATGTGGTTCTG

702 Reverse- CCGAGTTCGATGAACTGAGAG

703 *dOrai*:

704 Forward- GAGATAGCCATCCTGTGCTGG

705 Reverse- CGGATGCCCGAGACTGTC

706

707 **Immunohistochemistry**

708 Immunohistochemistry was performed on dissected adult CNS as described earlier
709 (7). Briefly, brains were dissected in 1x PBS, followed by fixation in 4%
710 paraformaldehyde and blocking in 0.2% phosphate buffer, 0.2% Triton-X 100 and
711 5% normal goat serum. Overnight incubation with primary antibodies was
712 followed by 2 hours of incubation with corresponding fluorescent secondary
713 antibodies. The primary antibodies used were: mouse anti TH (1:50, #22941,
714 ImmunoStar) and rabbit anti GFP (1:10,000, A6455, Life Technologies). The
715 following were the fluorescent secondary antibodies used at 1:400: anti-mouse
716 Alexa Fluor 568 (#A11004, Life Technologies) and anti-rabbit Alexa Fluor 488
717 (#A11008, Life Technologies). Images were obtained as confocal stacks of 1 μm
718 thickness using 20X objective on Olympus FV1000 Confocal microscope.

719 **Primary neuronal culture and immunostaining**

720 Primary neuronal cultures and immunostaining of neurons was carried out as
721 described previously (34). Briefly, third instar larval CNS were dissected in
722 Schneider's medium containing 50 μg/ml Streptomycin (Invitrogen), 10 μg/ml
723 Amphotericin B (Invitrogen) and 50U/ml Penicillin (Invitrogen). Following this,
724 brains were subjected to 40 minutes of enzyme treatment in 0.75 μg/ml
725 Collagenase and 0.40 μg/ml Dispase. Neurons were dissociated, spun down and
726 plated in growth medium, DMEM/F12-1065 (Gibco) supplemented with the

727 antibiotics mentioned previously and 20mM HEPES. All cell culture reagents were
728 procured from Sigma-Aldrich, unless specified differently. Fourteen-sixteen hours
729 old cultures were washed twice with hemolymph-like saline, HL_3 and incubated
730 with either the FMRFa peptide or a solvent control for 20 minutes. Following this,
731 cells were fixed in 3.5% paraformaldehyde for 20 minutes at room temperature and
732 then washed in wash buffer (1/10th dilution of blocking buffer). Cells were then
733 permeabilized for a total of half an hour (10 minutes * 3 times), blocked in
734 blocking buffer (5% BSA, 0.5% Triton X in PBS) for 1 hour, at room temperature
735 and subsequently incubated overnight in the primary antibody diluted in wash
736 buffer (mouse anti pCaMKII-22B1; 1:100; #sc-32289, Santa Cruz). The next day,
737 cells were washed thrice in wash buffer (for 10 minutes each) and incubated with
738 anti-mouse Alexa Fluor 568 (#A11004, Life Technologies) secondary antibody for
739 half an hour at room temperature. Control dishes for the secondary antibody were
740 treated as the experimental dishes and were incubated with the fluorescent
741 secondary, but not the primary antibody. Following another set of three washes (15
742 minutes each) in wash buffer, cells were covered in 60% glycerol before imaging.
743 An inverted Olympus FV3000 confocal microscope with a 60X oil objective (1.42
744 NA), pinhole size 150 μm was used to image the cells. GFP and pCaMKII signals
745 were captured with 488 and 561 laser lines respectively. The same settings were
746 used to capture images from all experimental conditions, on any particular day of

747 imaging. The entire cell volumes of cells were captured as optical slices of 0.60 µm
748 thickness. Images were analyzed in Image J as described above. After applying
749 background subtraction, fluorescence values of pCaMKII were divided over GFP
750 values to obtain the ratios shown in S3G Fig.

751 **Data representation and analysis**

752 Origin (OriginLab, Northampton, MA) software was used for plotting raw data and
753 calculation of statistical significance. Raw data were tested for normality. A
754 Student t-test or an ANOVA statistical test was performed on normally distributed
755 data. Non-normal data were tested for statistical significance using the Mann-
756 Whitney U-test.

757 **Acknowledgments**

758 We thank Prof. Jean-Francois Ferveur for helping us set up the locomotor assay,
759 Trayambak Pathak for standardising protocols for the Arclight experiments and
760 Shlesha Richhariya for help with FACS sorting. We thank the Fly Facility at
761 NCBS for generating transgenic fly lines and Dr. Krishnamurthy and NCBS
762 Central Imaging and Flow Facility for help with confocal imaging and FACS. We
763 also thank the Bloomington *Drosophila* Stock Center (National Institutes of Health
764 P40OD018537) for several fly stocks used in this study.

765 **References**

766 1. van den Pol AN. Neuropeptide Transmission in Brain Circuits. Neuron
767 [Internet]. 2012;76(1):98–115. Available from:
768 http://dx.doi.org/10.1016/j.neuron.2012.09.014

769 2. Taghert PH, Nitabach MN. Peptide Neuromodulation in Invertebrate Model
770 Systems. Neuron [Internet]. 2012;76(1):82–97. Available from:
771 http://dx.doi.org/10.1016/j.neuron.2012.08.035

772 3. Griffith LC. Neuromodulatory control of sleep in Drosophila melanogaster:
773 Integration of competing and complementary behaviors. Curr Opin
774 Neurobiol. 2013;23(5):819–23.

775 4. Kim SM, Su C, Wang JW. Neuromodulation of Innate Behaviors in
776 Drosophila. Annu Rev Neurosci. 2017;40:327–48.

777 5. Brembs B, Christiansen F, Pflüger HJ, Duch C, Pfluger HJ, Duch C. Flight
778 Initiation and Maintenance Deficits in Flies with Genetically Altered
779 Biogenic Amine Levels. J Neurosci [Internet]. 2007;27(41):11122–31.
780 Available from:
781 http://www.jneurosci.org/cgi/doi/10.1523/JNEUROSCI.2704-07.2007

782 6. Agrawal T, Hasan G. Maturation of a central brain flight circuit in
783 Drosophila requires Fz2/Ca^{2+} signaling. Elife. 2015;4(MAY):1–22.

784 7. Pathak T, Agrawal T, Richhariya S, Sadaf S, Hasan G. Store-Operated
785 Calcium Entry through Orai Is Required for Transcriptional Maturation of
786 the Flight Circuit in Drosophila. J Neurosci [Internet]. 2015;35(40):13784–
787 99. Available from:
788 http://www.jneurosci.org/cgi/doi/10.1523/JNEUROSCI.1680-15.2015

789 8. Hewes RS, Taghert PH. Neuropeptides and Neuropeptide Receptors in the
790 *Drosophila melanogaster* Genome. Genome Biol. 2001;11:1126–42.

791 9. Mertens I, Vandingenen A, Johnson EC, Shafer OT, Li W, Trigg JS, et al.
792 PDF Receptor Signaling in Drosophila Contributes to Both Circadian and
793 Geotactic Behaviors. Neuron. 2005;48:213–9.

794 10. Yapici N, Kim Y, Ribeiro C, Dickson BJ. A receptor that mediates the post-
795 mating switch in Drosophila reproductive behaviour. Nature.
796 2008;451(January):33–8.

797 11. Chen X, Ganetzky B. A neuropeptide signaling pathway regulates synaptic
798 growth in Drosophila melanogaster. J Cell Biol. 2012;196(4):529–43.

799 12. Vecsey CG, Pírez N, Griffith LC. The Drosophila neuropeptides PDF and
800 sNPF have opposing electrophysiological and molecular effects on central
801 neurons. J Neurophysiol. 2014;111:1033–45.

802 13. Klose MK, Dason JS, Atwood HL, Boulianne GL, Mercier AJ. Peptide-
803 induced modulation of synaptic transmission and escape response in
804 Drosophila requires two G-protein-coupled receptors. J Neurosci [Internet].
805 2010;30(44):14724–34. Available from:
806 http://www.ncbi.nlm.nih.gov/pubmed/21048131

807 14. Agrawal T, Sadaf S, Hasan G. A Genetic RNAi Screen for IP3/Ca2+
808 Coupled GPCRs in Drosophila Identifies the PdfR as a Regulator of Insect
809 Flight. PLoS Genet. 2013;9(10):e1003849.

810 15. Jayakumar S, Richhariya S, Venkateswara Reddy O, Texada MJ, Hasan G.
811 Drosophila larval to pupal switch under nutrient stress requires IP3R/Ca2+
812 signalling in glutamatergic interneurons. Elife. 2016;5(AUGUST):1–27.

813 16. Berridge MJ. Inositol trisphosphate and calcium signalling mechanisms.
814 Biochim Biophys Acta - Mol Cell Res [Internet]. 2009;1793(6):933–40.
815 Available from: http://dx.doi.org/10.1016/j.bbamcr.2008.10.005

816 17. Nässel DR. Neuropeptides in the nervous system of Drosophila and other
817 insects : multiple roles as neuromodulators and neurohormones. Prog
818 Neurobiol. 2002;68:1–84.

819 18. Kiss B, Szlanka T, Zvara Á, Žurovec M, Sery M, Kakaš Š, et al. Selective
820 elimination/RNAi silencing of FMRF-related peptides and their receptors

821 decreases the locomotor activity in Drosophila melanogaster. Gen Comp
822 Endocrinol. 2013;191(June):137–45.

823 19. Lenz O, Xiong J, Nelson MD, Raizen DM, Williams JA. FMRFamide
824 signaling promotes stress-induced sleep in Drosophila. Brain Behav Immun
825 [Internet]. 2015;47(February):141–8. Available from:
826 http://www.ncbi.nlm.nih.gov/pubmed/25668617%5Cnhttp://ac.els-
827 cdn.com/S0889159115000124/1-s2.0-S0889159115000124-
828 main.pdf?_tid=cdb35ce4-3da4-11e6-939d-
829 00000aacb35e&acdnat=1467169051_dac4c8bdfd8d49f91ae3d79c3cdeeac5

830 20. Banerjee S, Lee J, Venkatesh K, Wu C-F, Hasan G. Loss of flight and
831 associated neuronal rhythmicity in inositol 1,4,5-trisphosphate receptor
832 mutants of Drosophila. J Neurosci [Internet]. 2004 Sep 8 [cited 2012 May
833 11];24(36):7869–78. Available from:
834 http://www.pubmedcentral.nih.gov/articlerender.fcgi?artid=1289272&tool=p
835 mcentrez&rendertype=abstract

836 21. Friggi-Grelin F, Coulom H, Meller M, Gomez D, Hirsh J, Birman S.
837 Targeted gene expression in Drosophila dopaminergic cells using regulatory
838 sequences from tyrosine hydroxylase. J Neurobiol. 2003;54(4):618–27.

839 22. Liu Q, Liu S, Kodama L, Driscoll MR, Wu MN. Two dopaminergic neurons

840 signal to the dorsal fan-shaped body to promote wakefulness in Drosophila.
841 Curr Biol. 2012;22(22):2114–23.

842 23. Sitaraman D, Zars M, Laferriere H, Chen Y, Sable-smith A, Kitamoto T, et
843 al. Serotonin is necessary for place memory in Drosophila. Proc Natl Acad
844 Sci. 2008;105(14):5579–84.

845 24. Kondo S, Ueda R. Highly Improved gene targeting by germline-specific
846 Cas9 expression in Drosophila. Genetics. 2013;195(3):715–21.

847 25. Chen T-W, Wardill TJ, Sun Y, Pulver SR, Renninger SL, Baohan A, et al.
848 Ultrasensitive fluorescent proteins for imaging neuronal activity. Nature
849 [Internet]. 2013;499(7458):295–300. Available from:
850 http://www.pubmedcentral.nih.gov/articlerender.fcgi?artid=3777791&tool=p
851 mcentrez&rendertype=abstract

852 26. Schneider LE, Taghert PH. Isolation and characterization of a Drosophila
853 gene that encodes multiple neuropeptides related to Phe-Met-Arg-Phe-NH2
854 (FMRFamide). Proc Natl Acad Sci U S A [Internet]. 1988 Mar [cited 2017
855 Apr 5];85(6):1993–7. Available from:
856 http://www.ncbi.nlm.nih.gov/pubmed/3162321

857 27. Nambu JR, Murphy-Erdosh C, Andrews PC, Feistner GJ, Scheller RH.
858 Isolation and characterization of a drosophila neuropeptide gene. Neuron

859 [Internet]. 1988 [cited 2017 Apr 5];1(1):55–61. Available from:
860 http://www.sciencedirect.com/science/article/pii/0896627388902097

861 28. McGuire SE, Le PT, Osborn AJ, Matsumoto K, Davis RL. Spatiotemporal
862 rescue of memory dysfunction in Drosophila. Science [Internet].
863 2003;302(5651):1765–8. Available from:
864 http://www.ncbi.nlm.nih.gov/pubmed/14657498

865 29. Dunn TW, Mercier AJ. Synaptic modulation by a Drosophila neuropeptide is
866 motor neuron-specific and requires CaMKII activity. Peptides. 2005;26:269–
867 76.

868 30. Park D, Coleman MJ, Hodge JJL, Budnik V, Griffith LC. Regulation of
869 Neuronal Excitability in Drosophila by Constitutively Active CaMKII. J
870 Neurobiol. 2002;24–42.

871 31. Griffith LC, Verselis LM, Aitken KM, Lei L. Inhibition of
872 Calcium/Calmodulin-Dependent Protein Kinase in Drosophila Disrupts
873 Behavioral Plasticity. Neuron. 1993;10:501–9.

874 32. Nesler KR, Starke EL, Boin NG, Ritz M, Barbee SA. Molecular and Cellular
875 Neuroscience Presynaptic CamKII regulates activity-dependent axon
876 terminal growth. Mol Cell Neurosci [Internet]. 2016;76:33–41. Available
877 from: http://dx.doi.org/10.1016/j.mcn.2016.08.007

878 33. Gillespie JM, Hodge JJL. CASK regulates CaMKII autophosphorylation in
879 neuronal growth, calcium signaling, and learning. Front Mol Neurosci
880 [Internet]. 2013;6(September):27. Available from:
881 http://www.pubmedcentral.nih.gov/articlerender.fcgi?artid=3769642&tool=p
882 mcentrez&rendertype=abstract

883 34. Deb BK, Pathak T, Hasan G. Store-independent modulation of Ca2+ entry
884 through Orai by Septin 7. Nat Commun [Internet]. 2016;7(May):11751.
885 Available from:
886 http://www.ncbi.nlm.nih.gov/pubmed/27225060%5Cnhttp://www.pubmedce
887 ntral.nih.gov/articlerender.fcgi?artid=PMC4894974

888 35. Kudo Y, Ogura A. Glutamate-induced increase in intracellular Ca2+
889 concentration in isolated hippocampal neurones. Br J Pharmacol.
890 1986;89(1):191–8.

891 36. Cao G, Platisa J, Pieribone VA, Raccuglia D, Kunst M, Nitabach MN.
892 Resource Genetically Targeted Optical Electrophysiology in Intact Neural
893 Circuits. Cell [Internet]. 2013;154(4):904–13. Available from:
894 http://dx.doi.org/10.1016/j.cell.2013.07.027

895 37. Hamada FN, Rosenzweig M, Kang K, Pulver SR, Ghezzi A, Jegla TJ, et al.
896 An internal thermal sensor controlling temperature preference in Drosophila.

897 Nature [Internet]. 2008;454(7201):217–20. Available from:
898 http://www.ncbi.nlm.nih.gov/pubmed/18548007

899 38. Chen X, Rahman R, Guo F, Rosbash M. Genome-wide identification of
900 neuronal activity-regulated genes in *Drosophila*. Elife [Internet]. 2016;5:1–
901 21. Available from: http://elifesciences.org/lookup/doi/10.7554/eLife.19942

902 39. Nitabach MN, Wu Y, Sheeba V, Lemon WC, Strumbos J, Zelensky PK, et al.
903 Electrical Hyperexcitation of Lateral Ventral Pacemaker Neurons
904 Desynchronizes Downstream Circadian Oscillators in the Fly Circadian
905 Circuit and Induces Multiple Behavioral Periods. J Neurosci [Internet].
906 2006;26(2):479–89. Available from:
907 http://www.jneurosci.org/content/26/2/479%5Cnhttp://www.jneurosci.org/co
908 ntent/26/2/479.full.pdf%5Cnhttp://www.ncbi.nlm.nih.gov/pubmed/16407545

909 40. Wu Y, Cao G, Pavlicek B, Luo X, Nitabach MN. Phase Coupling of a
910 Circadian Neuropeptide With Rest / Activity Rhythms Detected Using a
911 Membrane-Tethered Spider Toxin. PLoS Biol. 2008;6(11).

912 41. Kitamoto T. Conditional Modification of Behavior in Drosophila by Targeted
913 Expression of a Temperature-Sensitive shibire Allele in Defined Neurons. J
914 Neurobiol. 2000;47:81–92.

915 42. Budnik V, White K. Genetic dissection of dopamine and serotonin synthesis

916 in the nervous system of Drosophila melanogaster. J Neurogenet.
917 1987;4:309–14.

918 43. White K, Hurteau T, Punsal P. Neuropeptide-FMRFamide-Like
919 Immunoreactivity in Drosophila : Development and Distribution. J Comp
920 Neurol. 1986;247:430–8.

921 44. Taghert, Paul H., Schneider LE. Interspecific Comparison of a Drosophila
922 Neuropeptides Gene Encoding FMRFamide-related neuropeptides. J
923 Neurosci. 1990;10(6):1929–42.

924 45. Nichols R, Mccormick J, Lim I, I LC. Cellular Expression of the Drosophila
925 melanogaster FMRFamide Neuropeptide Gene Product. J Mol Neurosci.
926 1995;6:1–10.

927 46. Nichols R, Mccormick J, Cohen M, Howe E, Paisley K, Rosario C, et al.
928 Differential Processing of Neuropeptides Influences Drosophila Heart Rate. J
929 Neurogenet. 1999;13((1-2)):89–104.

930 47. Shih C-T, Sporns O, Yuan S-L, Su T-S, Lin Y-J, Chuang C-C, et al.
931 Connectomics-Based Analysis of Information Flow in the Drosophila Brain.
932 Curr Biol [Internet]. 2015;25(10):1249–58. Available from:
933 http://www.sciencedirect.com/science/article/pii/S096098221500336X

934 48. Sadaf S, Reddy OV, Sane SP, Hasan G. Neural control of wing coordination
935 in flies. Curr Biol. 2015;25(1):80–6.

936 49. Davie K, Janssens J, Koldere D, Pech U, Aibar S, Waegeneer D, et al. A
937 single-cell catalogue of regulatory states in the ageing Drosophila brain.
938 bioRxiv. 2017;1–28.

939 50. Croset V, Treiber CD, Waddell S. Cellular diversity in the Drosophila
940 midbrain revealed by single-cell transcriptomics. Elife. 2018;7:1–31.

941 51. Bradley SP, Chapman PD, Lizbinski KM, Daly KC, Dacks AM. A Flight
942 Sensory-Motor to Olfactory Processing Circuit in the Moth Manduca sexta.
943 Front Neural Circuits [Internet]. 2016;10(5):1–13. Available from:
944 http://ovidsp.ovid.com/ovidweb.cgi?T=JS&PAGE=reference&D=prem&NE
945 WS=N&AN=26909026

946 52. Venkiteswaran G, Hasan G. Intracellular Ca2+ entry and store-operated
947 Ca2+ entry are required in Drosophila neurons for flight. Proc Natl Acad Sci
948 U S A. 2009;106(25):10326–31.

949 53. Malik BR, Hodge JJL. CASK and CaMKII function in Drosophila memory.
950 Front Neurosci. 2014;8(June):1–7.

951 54. Hell JW. CaMKII: Claiming center stage in postsynaptic function and

952 organization. Neuron [Internet]. 2014;81(2):249–65. Available from:
953 http://dx.doi.org/10.1016/j.neuron.2013.12.024

954 55. Wang Z, Wilson GF, Griffith LC. Calcium / Calmodulin-dependent Protein
955 Kinase II Phosphorylates and Regulates the Drosophila Eag Potassium
956 Channel. J Biol Chem. 2002;277(27):24022–9.

957 56. Zhou Y, Schopperle WM, Murrey H, Jaramillo A, Dagan D, Griffith LC, et
958 al. A Dynamically Regulated 14 – 3 – 3 , Slob , and Slowpoke Potassium
959 Channel Complex in Drosophila Presynaptic Nerve Terminals. Neuron.
960 1999;22:809–18.

961 57. Jiang X, Lautermilch NJ, Watari H, Westenbroek RE, Scheuer T, Catterall
962 WA. Modulation of CaV2.1 channels by Ca2+/calmodulin- dependent
963 protein kinase II bound to the C-terminal domain. Proc Natl Acad Sci U S A.
964 2008;105(1).

965 58. Timmerman C, Suppiah S, Gurudatta B V, Yang J, Banerjee C, Sandstrom
966 DJ, et al. The Drosophila transcription factor Adf-1 (nalyot) regulates
967 dendrite growth by controlling FasII and Staufen expression downstream of
968 CaMKII and neural activity. J Neurosci [Internet]. 2013;33(29):11916–31.
969 Available from:
970 http://www.pubmedcentral.nih.gov/articlerender.fcgi?artid=3713729&tool=p

971 mcentrez&rendertype=abstract

972 59. Vonhoff F, Kuehn C, Blumenstock S, Sanyal S, Duch C. Temporal
973 coherency between receptor expression , neural activity and AP-1-dependent
974 transcription regulates Drosophila motoneuron dendrite development.
975 Development. 2013;616:606–16.

976 60. Venkatesh K, Siddhartha G, Joshi R, Patel S, Hasan G. Interactions Between
977 the Inositol 1,4,5-Trisphosphate and Cyclic AMP Signaling Pathways
978 Regulate Larval Molting in Drosophila. Genetics. 2001;158(May):309–18.

979 61. Cong L, Ran FA, Cox D, Lin S, Barretto R, Habib N, et al. Multiplex
980 genome engineering using CRISPR/Cas systems. Science. 2013
981 Feb;339(6121):819–23.

982 62. Hsu PDD, Lander ESS, Zhang F. Development and applications of CRISPR-
983 Cas9 for genome engineering. Cell. 2014;157(6):1262–78.

984 63. Mali P, Yang L, Esvelt KM, Aach J, Guell M, DiCarlo JE, et al. RNA-guided
985 human genome engineering via Cas9. Science. 2013 Feb;339(6121):823–6.

986 64. Hwang WY, Fu Y, Reyon D, Maeder ML, Tsai SQ, Sander JD, et al.
987 Efficient genome editing in zebrafish using a CRISPR-Cas system. Nat
988 Biotechnol. 2013 Jan;31(3):227–9.

989 65. Sternberg SH, Doudna JA. Expanding the Biologist's Toolkit with CRISPR-
990 Cas9. Mol Cell. 2015;58(4):568–74.

991 66. Port F, Chen H-M, Lee T, Bullock SL. Optimized CRISPR/Cas tools for
992 efficient germline and somatic genome engineering in *Drosophila*. Proc Natl
993 Acad Sci U S A [Internet]. 2014;111(29):E2967-2976. Available from:
994 http://www.pubmedcentral.nih.gov/articlerender.fcgi?artid=4115528&tool=p
995 mcentrez&rendertype=abstract

996 67. Balakireva M, Stocker RF. Voila , a New Drosophila Courtship Variant that
997 Affects the Nervous System : Behavioral , Neural , and Genetic
998 Characterization. J Neurosci. 1998;18(11):4335–43.

999 68. Makos MA, Kim YC, Han KA, Heien ML, Ewing AG. In vivo
1000 electrochemical measurements of exogenously applied dopamine in
1001 Drosophila melanogaster. Anal Chem. 2009;81(5):1848–54.

1002 **Figure Legends**

1003 **Fig 1. FMRFaR on dopaminergic neurons is required for flight.** (A) Box plot
1004 showing duration of flight bouts in flies expressing $FMRFaR^{RNAi}$ in the indicated
1005 neuronal domains (red). In every box plot, the limits extend from 25th to 75th
1006 percentile, the line and solid diamond represent the median and mean respectively
1007 and the open diamonds show the individual data points. Significance was

1008 calculated by comparing with either the control genotypes (*FMRFaR*^{RNAi}/+,
1009 *nSyb/+, TH/+, THD1/+*) or as indicated by horizontal lines above the graph (n≥30,
1010 **p<0.01, Mann-Whitney U-test). Genotypic controls have been obtained
1011 throughout by crossing the strains to be tested with wild-type, *Canton-S*. The '+' in
1012 all control genotypes denotes the wild-type allele. (B) Quantitative PCR validation
1013 of *FMRFaR* knockdown in *nSyb* positive neurons. Each bar represents mean of
1014 normalized fold change ± SEM (n=6, One-way ANOVA followed by post-hoc
1015 Tukey's test; the same alphabet above each bar represents statistically
1016 indistinguishable groups; different alphabet represents p<0.01). (C) Snapshots of
1017 flight videos of the indicated genotypes (*FMRFaR*^{RNAi}*/+ and THD1>FMRFaR*^{RNAi})
1018 at time points before and after air-puff stimulus (green arrow). Flies of the control
1019 genotype continued to fly for time periods beyond those shown in the images. (D)
1020 Representation of the *FMRFaR* gene locus. The CRISPR-Cas9 based deletion
1021 removes ~1500 bp of the 1650 bp coding sequence. Primers used to amplify the
1022 5' (pink: 5'F, 5'R) and 3' (green: 3'F, 3'R) ends of the gene are indicated by
1023 arrows. Agarose gel showing PCR products from wild-type, heterozygous and
1024 homozygous knockouts of *FMRFaR*. L denotes DNA Ladder. (E) Quantitative
1025 PCR validation of *FMRFaR* CRISPR knockout from adult brains (n≥3, **p<0.01,
1026 unpaired t-test). (F) Flight bout duration of flies with CRISPR-Cas9 based

1027 knockout of *FMRFaR*. Statistical comparisons are as indicated by horizontal lines
1028 (n≥30, **p<0.01, Mann-Whitney U-test).

1029 **Fig 2. FMRFaR is expressed on dopaminergic neurons and is functionally**
1030 **active.** (A) Quantitative PCR on FACS sorted dopaminergic (GFP +ve, TH) and
1031 non-dopaminergic (GFP –ve, non TH) neurons, shows enrichment of *FMRFaR*
1032 transcripts in dopaminergic neurons. Each bar represents normalized fold change
1033 as mean ± SEM (n≥4, *p<0.05, unpaired t-test) (B) Snap shots of GCaMP6m
1034 responses from the indicated genotypes. The red box represents the magnified
1035 region of the protocerebrum shown in subsequent images. Warmer colors denote
1036 increase in [Ca^{2+}]. Scale bars indicate 20 μm. (C, D) Mean traces (±SEM) of
1037 normalized GCaMP6m fluorescence responses (ΔF/F) in *THD1GAL4* marked cells
1038 upon peptide or solvent addition (green arrow). (E) Area under the curve and (F)
1039 Peak ΔF/F quantified from 0 s to 420 s in (C, D). The box plot limits extend from
1040 25th to 75th percentile. The line and solid diamond represent the median and mean
1041 respectively. Individual data points are shown as open diamonds. Numbers below
1042 indicate total number of cells imaged. Each bar is compared to the Control peptide
1043 stimulated condition shown in black (**p<0.01; ns - not significant; Mann-
1044 Whitney U-test).

1045 **Fig 3. FMRFaR is required in adult dopaminergic neurons for sustained**
1046 **flight.** (A) Box plot showing flight bout durations by temporal knockdown of
1047 *FMRFaR* in *THD1* neurons using the TARGET system
1048 (*THD1;TubGAL80^{ts}>FMRFaR^{RNAi}*), which allows effective expression of
1049 transgene at 29°C, but not at 18°C. Animals maintained at 18°C or 29°C
1050 throughout development and as adults are indicated as 18°C and 29°C,
1051 respectively. Knockdown of *FMRFaR* only during the larval, pupal or adult stages
1052 are shown as 29°C Larval, 29°C Pupal or 29°C Adult, respectively (red).
1053 Knockdown of *FMRFaR* in adult stages (29°C Adult) reduced flight bout durations
1054 significantly. The phenotype observed upon *FMRFaR* knockdown in adults for 8
1055 days could be rescued by overexpression of the *itpr*$^{+}$ transgene, but not with
1056 another UAS transgene, *GCaMP6m* (*THD1;TubGAL80^{ts}>FMRFaR^{RNAi};itpr*$^{+}$
1057 shown in blue and *THD1;TubGAL80^{ts}>FMRFaR^{RNAi};GCaMP6m* shown in orange;
1058 n≥30, **p<0.01, ns – not significant; Mann-Whitney U-test). All comparisons are
1059 to the control condition, *THD1;TARGET>FMRFaR^{RNAi}* at 18°C (grey bar;
1060 *THD1;TubGAL80^{ts}>FMRFaR^{RNAi}*; 18°C) or as indicated by horizontal lines above
1061 the graph (n≥30, **p<0.01, Mann-Whitney U-test). (B) Immunohistochemistry of
1062 representative adult brain samples corresponding to 8 day adult controls (above;
1063 *THD1;TubGAL80^{ts}>mCD8GFP* Control) and *FMRFaR* knockdown (below;
1064 *THD1;TubGAL80^{ts}>mCD8GFP;FMRFaR^{RNAi}*). Anti-TH antibody was used to

1065 mark the various dopaminergic clusters, amongst which PPL1 and PPM3 clusters
1066 are indicated. Scale bars represent 100 µm. (C, D) Representative magnified views
1067 of the PPL1 (C) and PPM3 (D) clusters and their projections showing anti-GFP
1068 and anti-TH immunostaining in 8 day old adult brains of control (above;
1069 *THD1;TubGAL80^{ts}>mCD8GFP* Control) and *FMRFaR* knockdown (below;
1070 *THD1;TubGAL80^{ts}>mCD8GFP;FMRFaR^{RNAi}*). Scale bar represents 50 µm.

1071 **Fig 4. CaMKII function is required in dopaminergic neurons to regulate**
1072 **flight.** (A) Flight bout durations observed with overexpression of *WT-CaMKII* in
1073 the background of *FMRFaR* knockdown in *THD1* neurons
1074 (*THD1;TubGAL80^{ts}>WT-CaMKII;FMRFaR^{RNAi})*. A significant rescue of the flight
1075 defect was observed by expression in the adults, but not in pupae (n≥30, *p<0.05,
1076 **p<0.01, Mann-Whitney U-test). (B) Flight durations observed with expression of
1077 a genetically encoded CaMKII inhibitor peptide, *Ala*, in dopaminergic neurons as
1078 compared to *Ala* control (n≥30, **p<0.01, Mann-Whitney U-test). (C) Flight time
1079 of flies with temporal expression of *Ala* in *THD1* neurons using the TARGET
1080 system (*THD1;TubGAL80^{ts}>Ala*). Significant deficits in flight were observed upon
1081 CaMKII inhibition in pupal and adult stages as compared to flies maintained at
1082 18°C throughout (n≥30, **p<0.01, Mann-Whitney U-test). (D) Mean traces
1083 (±SEM) of normalized GCaMP6m responses in control (*THD1>GCaMP6m*) and
1084 *Ala* expressing *THD1* neurons (*THD1>GCaMP6m;Ala*) upon peptide stimulation

1085 (green arrow). (E) Area under the curve and (F) Peak ΔF/F quantified from 0 s to
1086 420 s in (D) were not significantly different between the two genotypes tested
1087 (p>0.05; ns - not significant; Mann-Whitney U-test).

1088 **Fig 5. Expression of *FMRFaR^{RNAi}* and inhibition of CaMKII in dopaminergic**
1089 **neurons reduces calcium entry after a depolarizing stimulus.** (A) Mean trace
1090 (±SEM) of normalized GCaMP6m responses observed upon KCl stimulation
1091 (green arrow) in 8 day adult neurons in the three indicated genotypes,
1092 *THD1;TubGAL80^{ts}>GCaMP6m, Control* in black;
1093 *THD1;TubGAL80^{ts}>GCaMP6m;FMRFaR^{RNAi},* in red and
1094 *THD1;TubGAL80^{ts}>GCaMP6m;Ala,* in blue. (B) Area under the curve and (C)
1095 Peak change in fluorescence quantified from (A). Each bar is compared to control
1096 shown in black (**p<0.01; Mann-Whitney U-test). (D) Snap shots of GCaMP6m
1097 responses from the same genotypes shown in (A). In the *FMRFaR^{RNAi}* knockdown
1098 condition (2nd row), the yellow arrow indicates a cell that responded whereas pink
1099 arrows indicate cells with no response or a minimal response to the depolarization
1100 stimulus. Scale bars represent 50 μm.

1101 **Fig 6. Expression of *FMRFaR^{RNAi}* in dopaminergic neurons reduces**
1102 **membrane depolarization.** (A) Mean trace (±SEM) of negative change in
1103 fluorescence (-ΔF/F) observed upon KCl stimulation of *THD1* neurons expressing
1104 a fluorescent-based membrane voltage indicator, *Arclight* in the indicated

1105 genotypes, *THD1;TubGAL80^{ts}>Arclight, Control* in black;
1106 *THD1;TubGAL80^{ts}>Arclight;FMRFaR^{RNAi},* in red. (B) Area under the curve and
1107 (C) Peak (-ΔF/F) quantified from (A) were significantly different in the *FMRFaR*
1108 knockdown neurons as compared to their genotypic controls. Numbers below each
1109 box plot indicate total number of cells imaged from a minimum of 5 independent
1110 brains (One-way ANOVA followed by post-hoc Tukey's test; the same alphabet
1111 above each bar represents statistically indistinguishable groups; different alphabet
1112 represents $p<0.05$). (D) Representative images of neuronal depolarization as
1113 observed by a decrease in Arclight fluorescence in the same genotypes shown in
1114 (A). With *FMRFaR* knockdown (2nd row), few cells responded normally (yellow
1115 arrow), whereas most others showed no response or a minimal response to the
1116 depolarization stimulus (pink arrow). Scale bars represent 50 µm. (E) Rescue of
1117 flight bout durations by expression of *dTrpA1* in the genetic background of
1118 *FMRFaR^{RNAi}* in 6 and 8 day old adult *THD1* marked neurons
1119 (*THD1;TubGAL80^{ts}>TrpA1;FMRFaR^{RNAi}* compared to
1120 *THD1;TubGAL80^{ts}>FMRFaR^{RNAi}*; $n\geq30$, **$p<0.01$, Mann-Whitney U-test).

1121 **Fig 7. Dopaminergic neurons require optimal membrane excitability and**
1122 **synaptic vesicle recycling for sustained flight**

1123 (A) Flight bout durations were significantly reduced upon adult specific expression
1124 of the Ca^{2+} channel inhibitor, *PLTXII* (*THD1;TubGAL80^{ts}>PLTXII;* $n\geq30$,

1125 **p<0.01, Mann-Whitney U-test). (B) Expression of a K^+ channel inhibitor, *κ-*
1126 *ACTX-Hv1c*, in adult dopaminergic neurons reduces flight bout durations
1127 (*THD1;TubGAL80^{ts}>κ-ACTX-Hv1c;* n≥30, **p<0.01, Mann-Whitney U-test). (C)
1128 Adult dopaminergic neuron specific expression of *δ-ACTX-Hv1a*, a toxin that
1129 targets Na^+ channels, significantly reduces flight bout durations
1130 (*THD1;TubGAL80^{ts}>δ-ACTX-Hv1a*; n≥30, **p<0.01, Mann-Whitney U-test). In
1131 all the above cases (A, B, C), comparisons have been made with the corresponding
1132 18°C control (black). (D) Acute expression of a temperature sensitive dynamin
1133 mutant (*Shi^{ts}*) in adult dopaminergic neurons reduced flight bout durations when
1134 tested at 30°C as compared to a control tested at 22°C (*THD1>Shi^{ts}* at 22°C
1135 compared to 30°C; n≥30, **p<0.01, Mann-Whitney U-test). *THD1/+* and *Shi^{ts}/+*
1136 controls in the two temperature conditions are also shown. (E) Adult specific
1137 knockdown of the dopamine synthesizing enzyme, Tyrosine Hydroxylase (*TH*) by
1138 expressing an RNAi (*TH^{RNAi}*) in dopaminergic neurons significantly reduces flight
1139 duration as compared to the corresponding 18°C controls
1140 (*THD1;TubGAL80^{ts}>TH^{RNAi};* n≥30, **p<0.01, Mann-Whitney U-test).

1141 **S1 Fig**. **Flight duration and locomotor activity measurements with *FMRFaR***
1142 **knockdown in subset dopaminergic neurons.** (A) Flight durations observed with
1143 knockdown of *FMRFaR* in a few TH subset domains, namely, *THD'*, *THC1* and
1144 *THC'* as compared to their genotypic controls (*THD'/+, THC1/+, THC'/+* in black

1145 and *FMRFaR*^{RNAi}/+ shown in Fig 1A; n≥30, **p<0.01, Mann-Whitney U-test). The
1146 '+' in all control genotypes denotes the wild-type, *Canton-S*, allele. (B) Locomotor
1147 activity measured for control adult flies (*THD1/+* and *FMRFaR*^{RNAi}/+) were not
1148 different from that observed with *THD1>FMRFaR*^{RNAi} flies (n=25, p>0.05, Mann-
1149 Whitney U-test).

1150 **S2 Fig**. **Behavior characterization under control conditions.** (A) Genotypic
1151 controls for the TARGET experiment (*FMRFaR*^{RNAi}/+ and *THD1;TubGAL80*^{ts}
1152 *Control*) tested for flight under various temperature shift conditions. Other controls
1153 in the graph include *itpr*$^{+}$/+;*FMRFaR*^{RNAi}/+ (4th bar from the left in black),
1154 *THD1;TubGAL80*^{ts}*>itpr*$^{+}$ (orange bar) and *THD1;TubGAL80*^{ts}*>cas9* (pink bar).
1155 Comparisons are shown by horizontal lines (n=30, **p<0.01, ns – not significant;
1156 Mann-Whitney U-test). (B) Immunohistochemical staining of 8 day old adult
1157 brains using anti-GFP antibody in control (above; *THD1;TubGAL80*^{ts}*>mCD8GFP*
1158 Control) and *FMRFaR* knockdown (below;
1159 *THD1;TubGAL80*^{ts}*>mCD8GFP;FMRFaR*^{RNAi}) conditions. Scale bars represent
1160 100 μm.

1161 **S3 Fig. Behavioral and molecular characterization of CaMKII and *Ala* strains**
1162 **under various behavioral paradigms.** (A) Flight durations observed for a strain
1163 used in Fig 4A (*WT-CaMKII/+;FMRFaR*^{RNAi}/+). Flight bout durations measured

1164 for flies with expression of *WT-CaMKII* (*THD1;TubGAL80^{ts}>WT-CaMKII*) or a
1165 constitutively active form of CaMKII, *CaMKII^{T287D}*
1166 (*THD1;TubGAL80^{ts}>CaMKII^{T287D}*), in *THD1* marked neurons under various
1167 temperature shift conditions as compared to the 18°C condition (n≥20, **p<0.01,
1168 Mann-Whitney U-test). (B) Flight bout durations observed with knockdown of
1169 *CaMKII* (*CaMKII^{RNAi}*) in dopaminergic neurons (n≥30, *p<0.05, **p<0.01, Mann-
1170 Whitney U-test). (C) Locomotor activity of control adult flies and flies with *THD1*
1171 driven *Ala* expression (*Ala/+* and *THD1>Ala*; n=25, p>0.05, ns - not significant;
1172 Mann-Whitney U-test). (D) Flight bout durations observed with an *Ala* control
1173 strain under the various temperature shift conditions (*Ala/+*; n≥20). (E)
1174 Quantitative PCR showing normalized mean fold change (± SEM) in *TH*
1175 transcripts under conditions of *Ala* expression in *THD1* neurons, either in pupae or
1176 adults (*THD1;TubGAL80^{ts} Control* and *THD1;TubGAL80^{ts}>Ala*; n≥3, p>0.05,
1177 unpaired t-test). (F) Box plot showing background subtracted fluorescence
1178 intensity values of GFP and anti-pCaMKII under various experimental conditions.
1179 Cells with GFP intensities ranging from 0-1500 units were chosen for analysis and
1180 their distributions were not different in the three conditions
1181 (*nsyb>mCD8GFP;FMRFaR^{+};* p>0.05, ns - not significant; Mann-Whitney U-test).
1182 (G) Box plot showing the ratio of pCaMKII/GFP fluorescence intensity in the three
1183 experimental conditions. Peptide stimulation resulted in significantly higher

1184 pCaMKII/GFP ratios as compared to addition of the solvent (**p<0.01, Mann-
1185 Whitney U-test). (H) Representative images of cells showing endogenous GFP and
1186 staining for pCaMKII in the three treatment groups. Scale bar represents 10 µm.

1187 **S4 Fig. GCaMP6m imaging of *THD1* neurons after *FMRFaR* knockdown for**
1188 **2 days in adults.** (A) GCaMP6m traces showing normalized mean response
1189 (±SEM) of *THD1* neurons to KCl in 2 day old adult brains of the indicated
1190 genotypes, *THD1;TubGAL80^{ts}>GCaMP6m, Control* in black;
1191 *THD1;TubGAL80^{ts}>GCaMP6m;FMRFaR^{RNAi},* in red. (B) Area under the curve
1192 and (C) Peak ΔF/F quantified from (A). Numbers below each box plot indicate
1193 total number of cells imaged (*p<0.05; Mann-Whitney U-test).

1194 **S5 Fig. Cellular and behavioral characterization under control conditions** (A)
1195 Mean – ΔF/F traces observed in 2 day old adult dopaminergic neurons in response
1196 to KCl stimulation, where *THD1* neurons express the *Arclight* transgene in the
1197 indicated genotypes, *THD1;TubGAL80^{ts}>Arclight, Control* in black;
1198 *THD1;TubGAL80^{ts}>Arclight;FMRFaR^{RNAi},* in red,
1199 *THD1;TubGAL80^{ts}>Arclight;Kir2.1* in blue. (B) Area under the curve and (C)
1200 Peak – (ΔF/F) calculated from (A). Expression of the hyperpolarizing channel,
1201 *Kir2.1*, significantly reduced the response to a depolarizing KCl stimulus. Numbers
1202 below each box plot indicate total number of cells imaged (One-way ANOVA
1203 followed by post-hoc Tukey's test; the same alphabet above each bar represents

statistically indistinguishable groups; different alphabet represents $p<0.01$). (D) Flight durations observed for flies expressing just the *TrpA1* transgene in adult *THD1* neurons as compared to 18°C control (*THD1;TubGAL80^{ts}>TrpA1;* $n\geq20$, **$p<0.01$, Mann-Whitney U-test). Flight duration of a control genotype used in Fig 6E (*TrpA1/+;FMRFaR^{RNAi}/+* - black bar). (E) Rescue of flight deficits observed upon expression of *NaChBac*, in the background of CaMKII inhibition (*Ala*) in *THD1* neurons in 6 and 8 day old adults (*THD1;TubGAL80^{ts}>Ala;NaChBac* compared to *THD1;TubGAL80^{ts}>Ala*; $n\geq30$, *$p<0.05$, **$p<0.01$, Mann-Whitney U-test). The rescues are presumably due to increased membrane excitability. (F) Flight bout durations observed with expression of just the *NaChBac* transgenes in *THD1* neurons under control condition (18°C) and for 6 or 8 days as adults (*THD1;TubGAL80^{ts}>NaChBac*; orange bars; $n\geq20$, **$p<0.01$, Mann-Whitney U-test). Flight times observed with expression of a *GCaMP6m* transgene in the background of *Ala* expression in adult *THD1* neurons (*THD1;TubGAL80^{ts}>Ala;GCaMP6m*; green bar compared to *THD1;TubGAL80^{ts}>Ala,* 8 days as adults at 29°C shown in Fig 4C are not significantly different; $n\geq20$, $p>0.05$, Mann-Whitney U-test). Flight duration of a control genotype used in Fig 6E (*Ala/+;NaChBac/+* - black bar).

S6 Fig. Behavioral and cellular characterization with channel toxin transgenes. (A) Flight times observed for controls of the three channel toxin

1224 transgenes (*PLTXII/+, κ-ACTX-Hv1c/+ and δ-ACTX-Hv1a/+*; n≥30, Mann-
1225 Whitney U-test). (B) Anti-TH immunostaining of 4 day old adult brains expressing
1226 the various channel toxin transgenes (*THD1;TubGAL80^{ts}>PLTXII,*
1227 *THD1;TubGAL80^{ts}>κ-ACTX-Hv1c and THD1;TubGAL80^{ts}>δ-ACTX-Hv1a)*.
1228 Neurons in various dopaminergic clusters were intact. Scale bars represent 100 μm.
1229 (C) Proposed signaling mechanism in dopaminergic neurons for regulation of
1230 flight bout durations by FMRFaR. The model illustrates that FMRFaR stimulation
1231 and downstream IP_3R-mediated Ca^{2+} release could possibly activate CaMKII. Our
1232 data suggest that the FMRFaR and CaMKII are required in dopaminergic neurons
1233 for optimal membrane excitability. The effect on membrane excitability maybe by
1234 direct modification of membrane channels or by regulation of their expression
1235 levels. We further predict that this excitability is required for exocytosis of
1236 dopamine containing synaptic vesicles. Schematics are not drawn to scale.

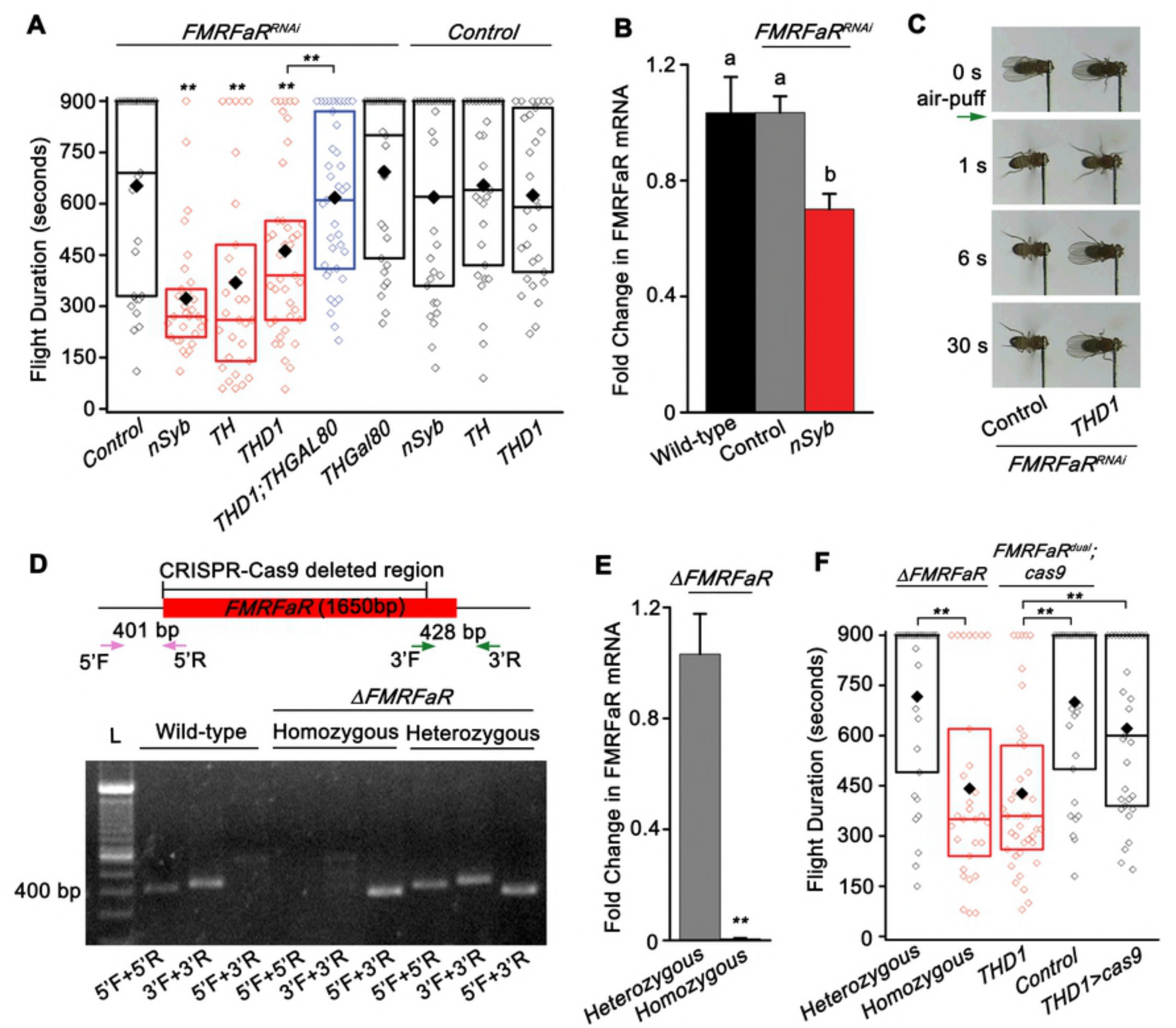
A
FMRFaR^RNAi
Control
Flight Duration (seconds)
900
750
600
450
300
150
0
**
Control
nSyb
TH
THD1
THD1;THGAL80
THGal80
nSyb
TH
THD1
B
FMRFaR^RNAi
Fold Change in FMRFaR mRNA
1.2
0.8
0.4
0
a
a
b
Wild-type
Control
nSyb
C
0 s
air-puff
1 s
6 s
30 s
Control
THD1
FMRFaR^RNAi
D
CRISPR-Cas9 deleted region
FMRFaR (1650bp)
401 bp
428 bp
5'F
5'R
3'F
3'R
ΔFMRFaR
L
Wild-type
Homozygous
Heterozygous
400 bp
5'F+5'R
3'F+3'R
5'F+3'R
5'F+5'R
3'F+3'R
5'F+3'R
5'F+5'R
3'F+3'R
5'F+3'R
E
ΔFMRFaR
Fold Change in FMRFaR mRNA
1.2
0.8
0.4
0
**
Heterozygous
Homozygous
F
ΔFMRFaR
FMRFaR^dual; cas9
Flight Duration (seconds)
900
750
600
450
300
150
0
**
**
**
Heterozygous
Homozygous
THD1
Control
THD1>cas9

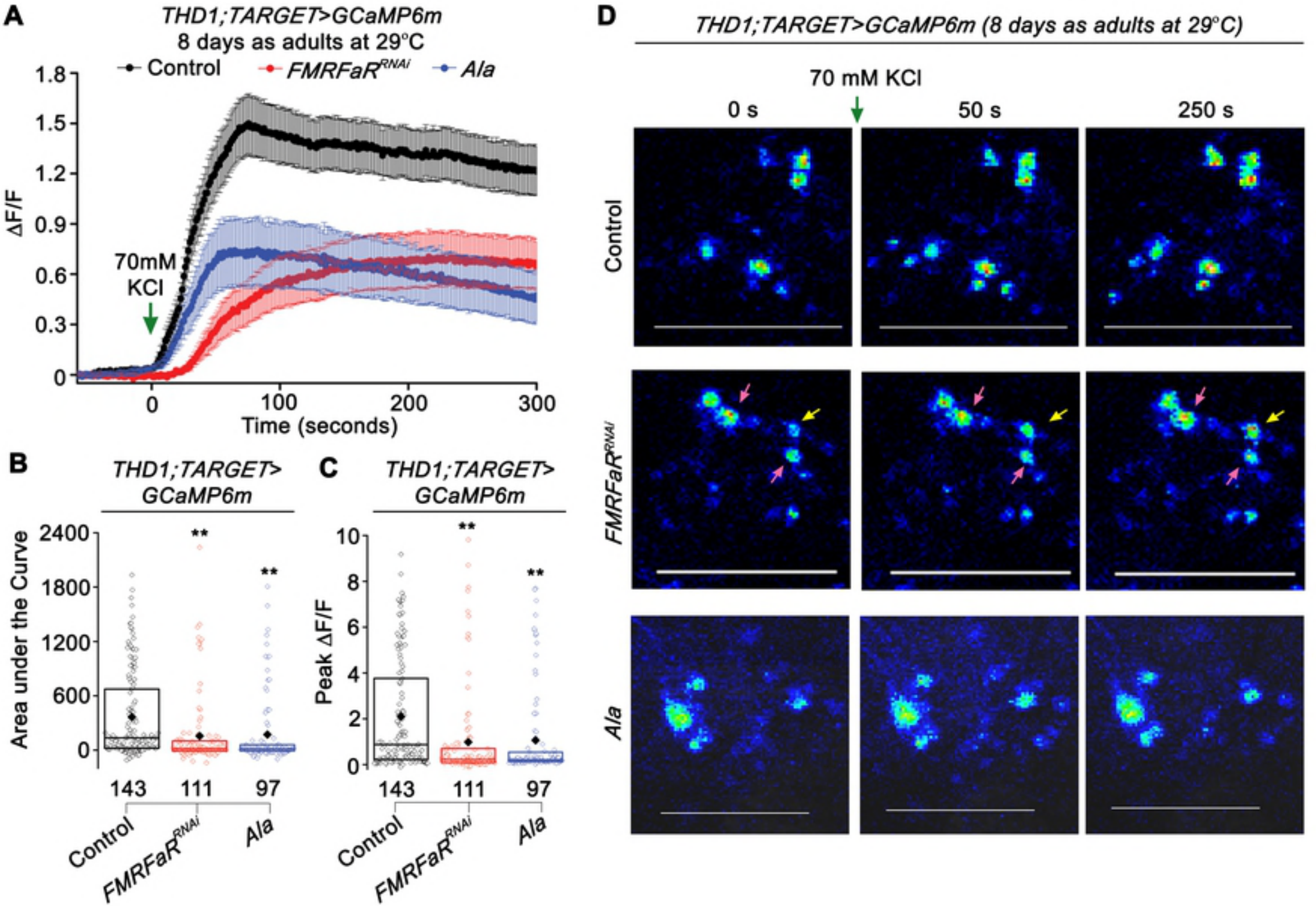
A
THD1;TARGET>GCaMP6m
8 days as adults at 29°C
Control
FMRFaR^RNAi
Ala
ΔF/F
70mM KCl
Time (seconds)
B
THD1;TARGET> GCaMP6m
Area under the Curve
143
111
97
Control
FMRFaR^RNAi
Ala
C
THD1;TARGET> GCaMP6m
Peak ΔF/F
143
111
97
Control
FMRFaR^RNAi
Ala
D
THD1;TARGET>GCaMP6m (8 days as adults at 29°C)
70 mM KCl
0 s
50 s
250 s
Control
FMRFaR^RNAi
Ala

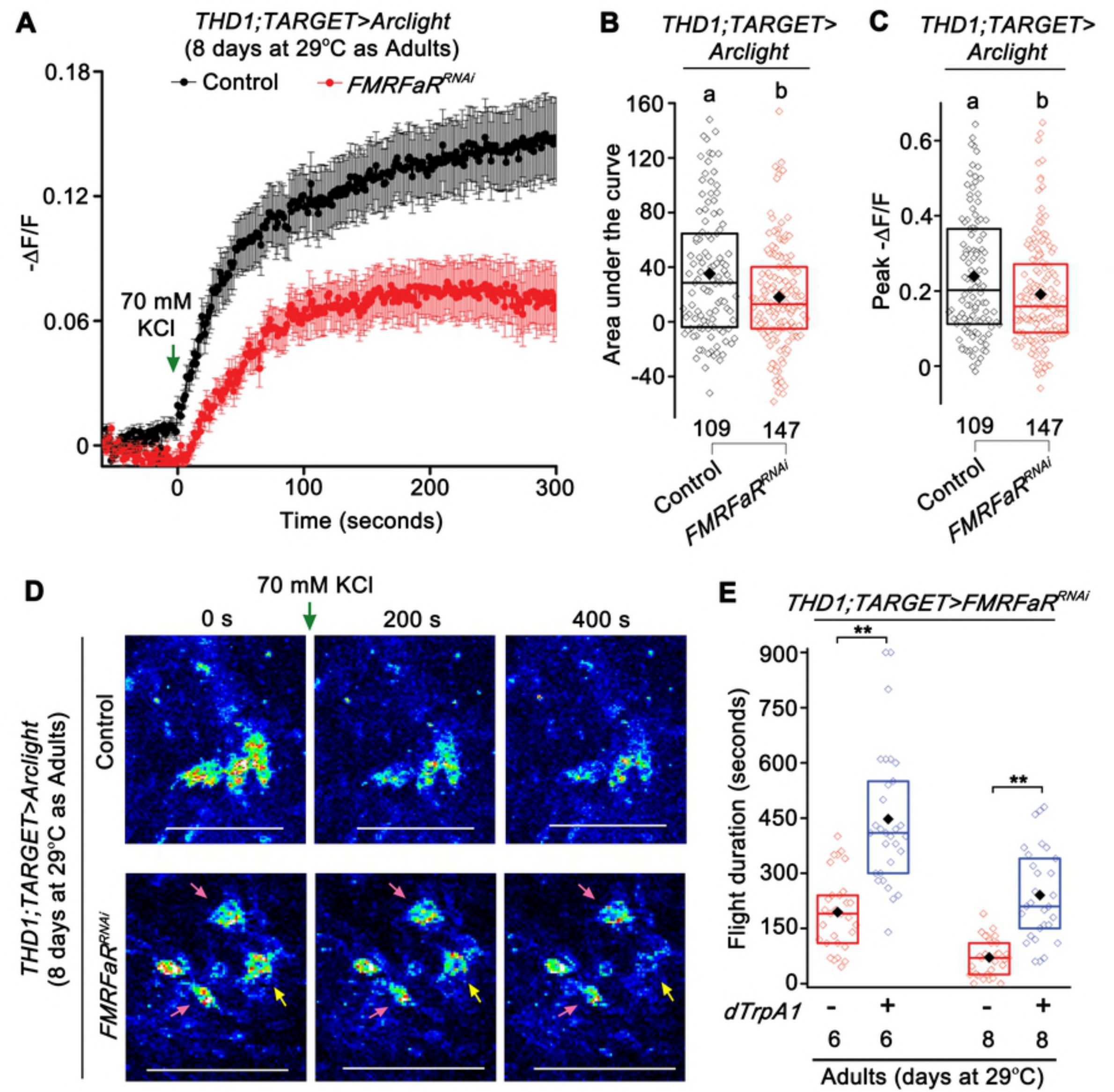
A
THD1;TARGET>Arclight
(8 days at 29°C as Adults)
Control
FMRFaR^RNAi
-ΔF/F
0.18
0.12
0.06
0
70 mM
KCl
0
100
200
300
Time (seconds)
B
THD1;TARGET>
Arclight
Area under the curve
160
120
80
40
0
-40
a
b
109
147
Control
FMRFaR^RNAi
C
THD1;TARGET>
Arclight
Peak -ΔF/F
0.6
0.4
0.2
0
a
b
109
147
Control
FMRFaR^RNAi
D
70 mM KCl
0 s
200 s
400 s
THD1;TARGET>Arclight
(8 days at 29°C as Adults)
Control
FMRFaR^RNAi
E
THD1;TARGET>FMRFaR^RNAi
Flight duration (seconds)
900
750
600
450
300
150
0
**
**
dTrpA1
-
+
-
+
6
6
8
8
Adults (days at 29°C)

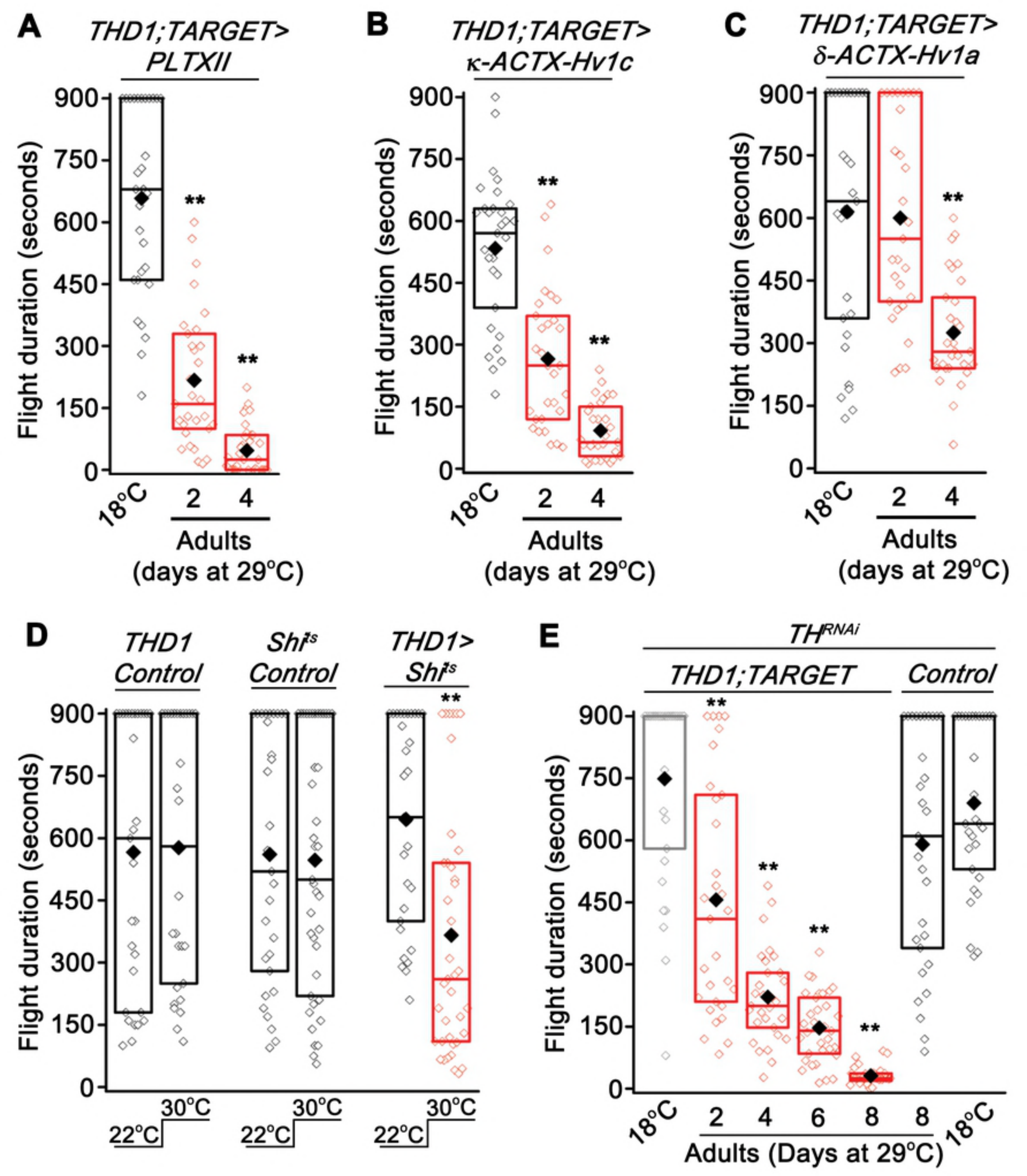
A
THD1;TARGET>
PLTXII
B
THD1;TARGET>
κ-ACTX-Hv1c
C
THD1;TARGET>
δ-ACTX-Hv1a
Flight duration (seconds)
900
750
600
450
300
150
0
**
18°C
2
4
Adults
(days at 29°C)
D
THD1
Control
Shi^ts
Control
THD1>
Shi^ts
22°C
30°C
E
TH^RNAi
THD1;TARGET
Control
6
8
18°C

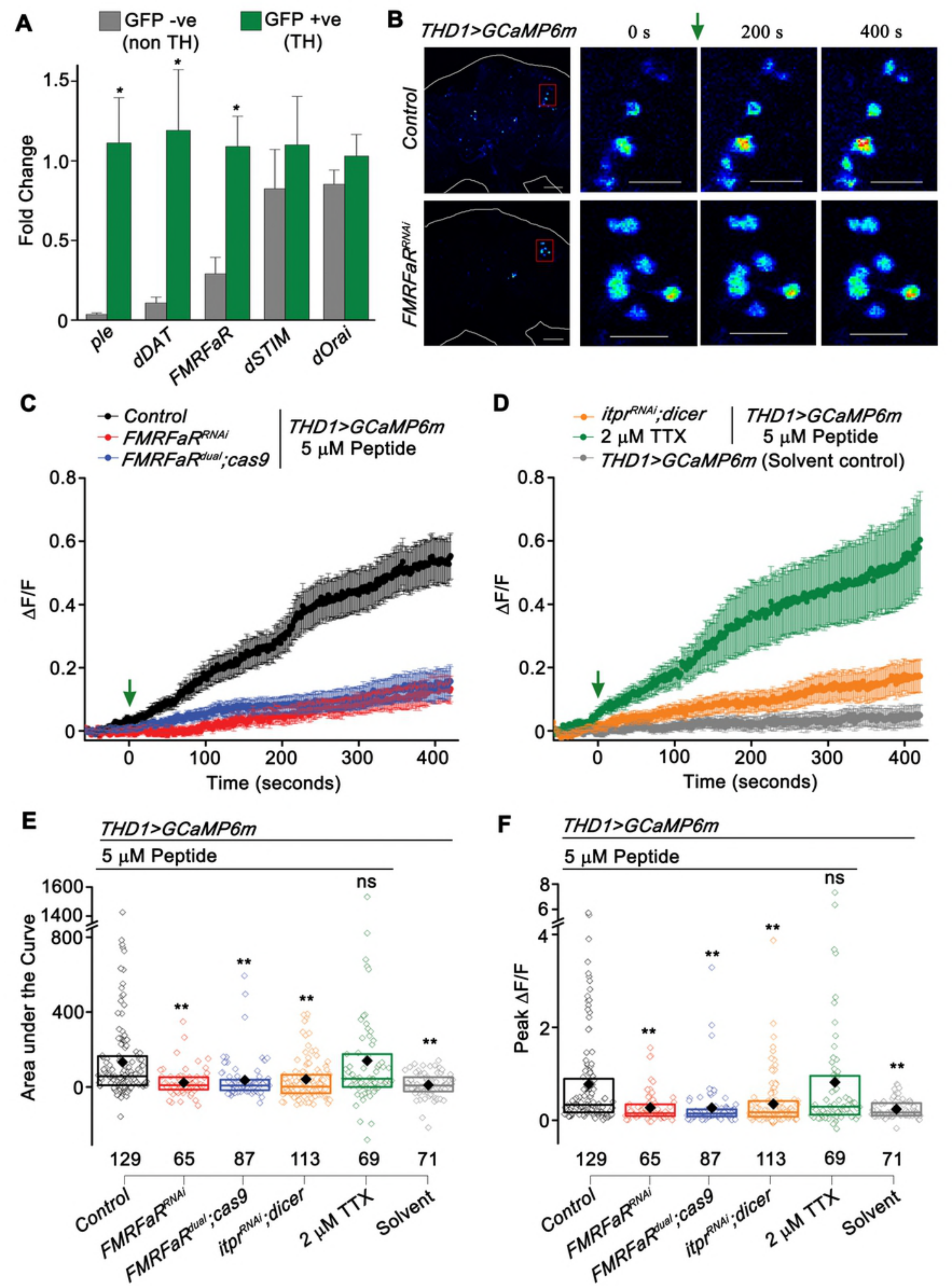
A
GFP -ve (non TH)
GFP +ve (TH)
Fold Change
ple
dDAT
FMRFaR
dSTIM
dOrai
B
THD1>GCaMP6m
0 s
200 s
400 s
Control
FMRFaR RNAi
C
Control
FMRFaR RNAi
FMRFaR dual;cas9
THD1>GCaMP6m
5 μM Peptide
ΔF/F
Time (seconds)
D
itpr RNAi;dicer
2 μM TTX
THD1>GCaMP6m
5 μM Peptide
THD1>GCaMP6m (Solvent control)
ΔF/F
Time (seconds)
E
THD1>GCaMP6m
5 μM Peptide
Area under the Curve
ns
129
65
87
113
69
71
Control
FMRFaR RNAi
FMRFaR dual;cas9
itpr RNAi;dicer
2 μM TTX
Solvent
F
THD1>GCaMP6m
5 μM Peptide
Peak ΔF/F
ns
129
65
87
113
69
71
Control
FMRFaR RNAi
FMRFaR dual;cas9
itpr RNAi;dicer
2 μM TTX
Solvent

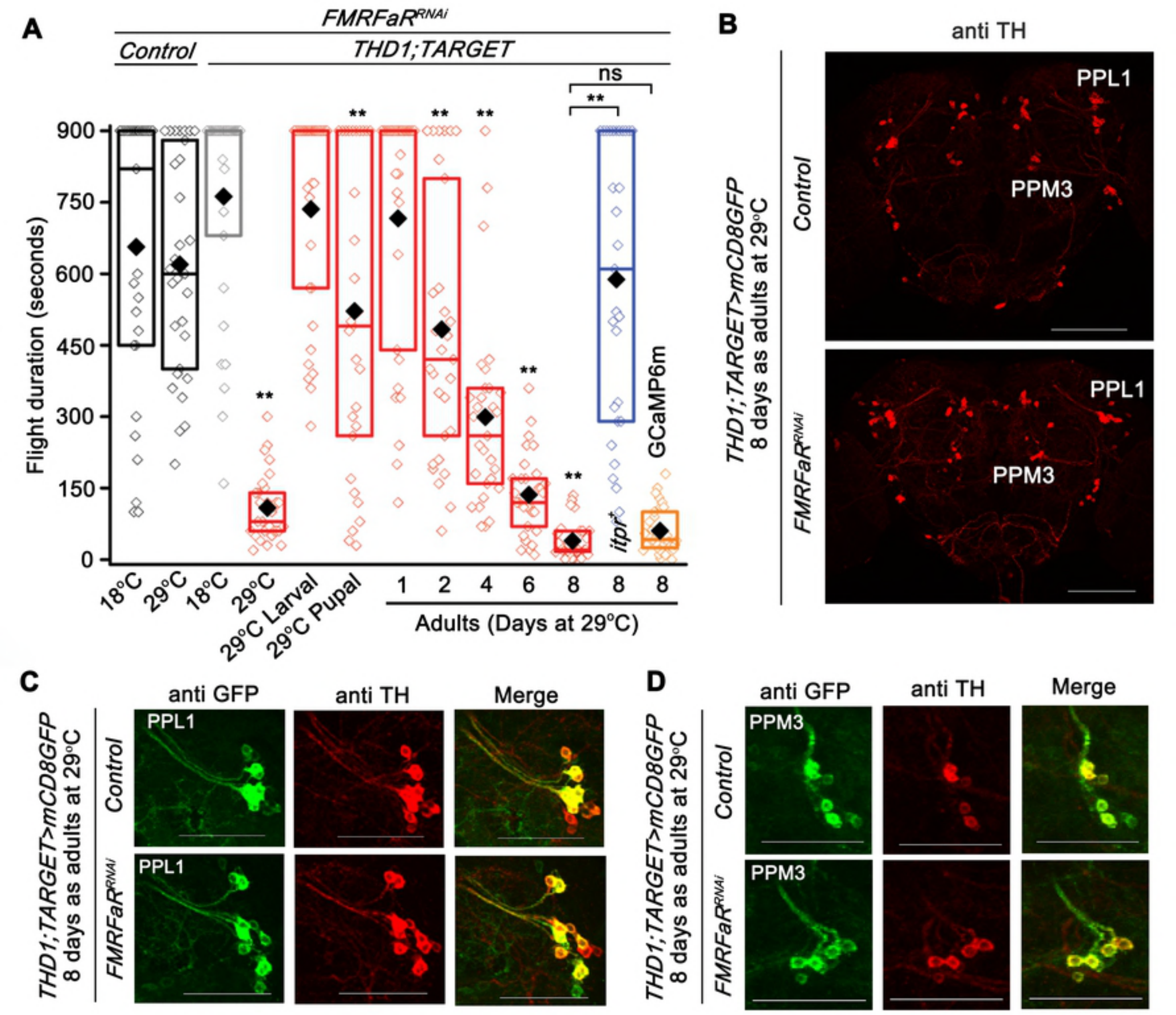
A
FMRFaR^RNAi
Control
THD1;TARGET
ns
**
Flight duration (seconds)
900
750
600
450
300
150
0
GCaMP6m
itpr
18°C
29°C
18°C
29°C
29°C Larval
29°C Pupal
1
2
4
6
8
8
8
Adults (Days at 29°C)
B
anti TH
THD1;TARGET>mCD8GFP
8 days as adults at 29°C
Control
FMRFaR^RNAi
PPL1
PPM3
C
anti GFP
anti TH
Merge
D

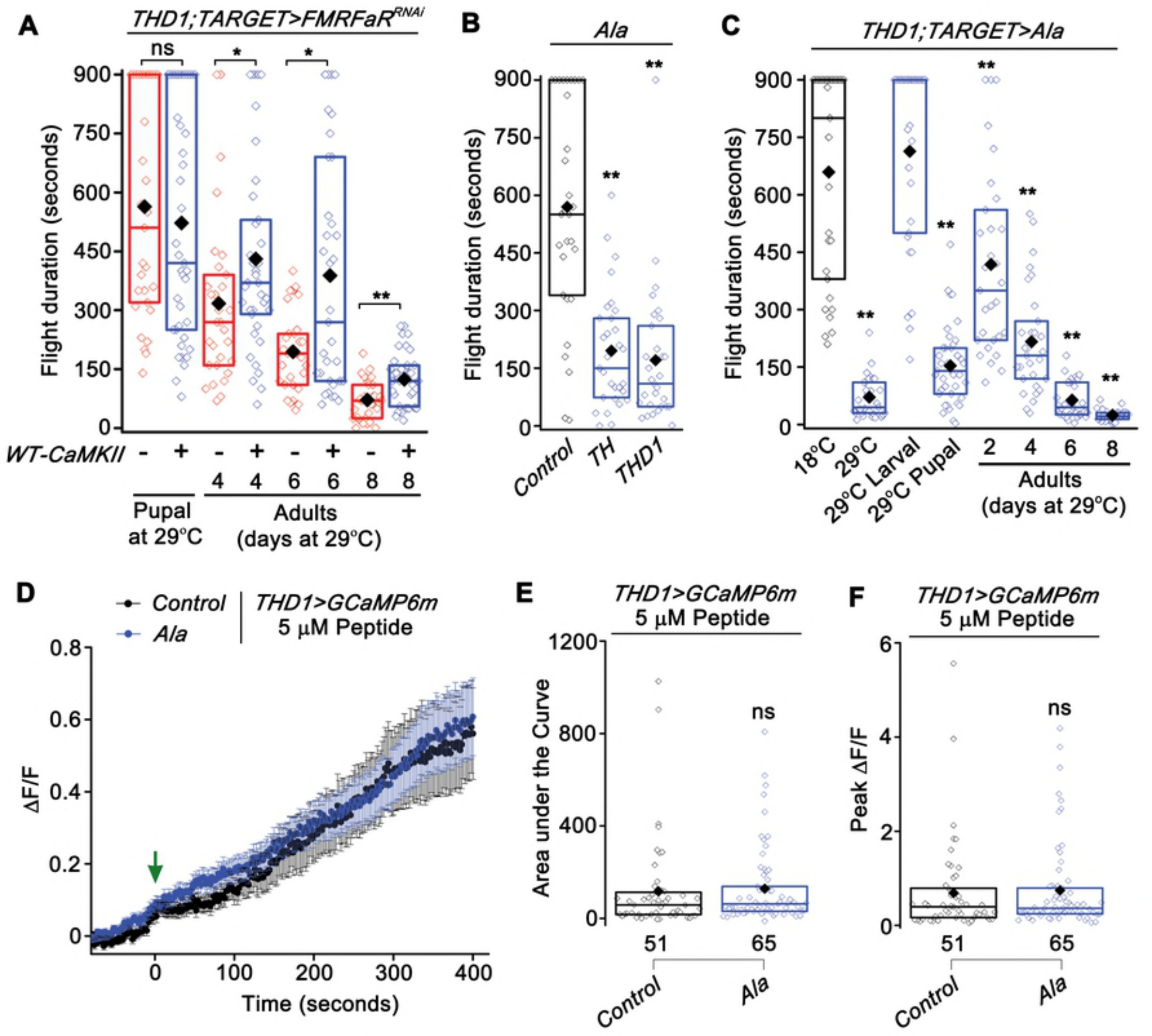
A
THD1;TARGET>FMRFaR^RNAi
Flight duration (seconds)
ns
*
*
**
WT-CaMKII - + - + - + - +
4 4 6 6 8 8
Pupal at 29°C
Adults (days at 29°C)
B
Ala
Control
TH
THD1
C
THD1;TARGET>Ala
18°C
29°C
29°C Larval
29°C Pupal
2 4 6 8
Adults (days at 29°C)
D
Control
Ala
THD1>GCaMP6m
5 μM Peptide
ΔF/F
Time (seconds)
E
THD1>GCaMP6m
5 μM Peptide
Area under the Curve
51
65
F
Peak ΔF/F